

# Radiolabeled Peptides and Antibodies in Medicine

Paweł Kręcisz, Kamila Czarnecka, Leszek Królicki, Elżbieta Mikiciuk-Olasik, and Paweł Szymański\*



Cite This: *Bioconjugate Chem.* 2021, 32, 25–42



Read Online

ACCESS |



Metrics & More

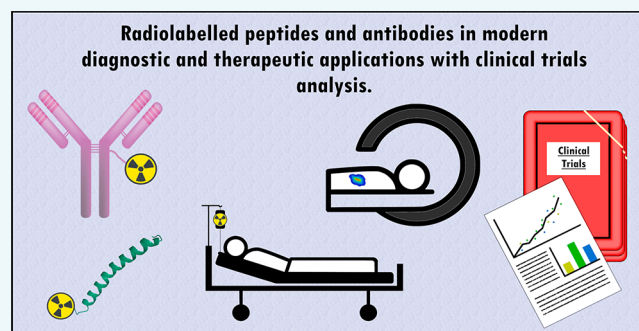


Article Recommendations



Supporting Information

**ABSTRACT:** Radiolabeled peptides are a relatively new, very specific radiotracer group, which is still expanding. This group is very diverse in terms of peptide size. It contains very small structures containing several amino acids and whole antibodies. Moreover, radiolabeled peptides are diverse in terms of the binding aim and therapeutic or diagnostic applications. The majority of this class of radiotracers is utilized in oncology, where the same structure can be used in therapy and diagnostic imaging by varying the radionuclide. In this study, we collected new reports of radiolabeled peptide applications in diagnosis and therapy in oncology and other fields of medicine. Radiolabeled peptides are also increasingly being used in rheumatology, cardiac imaging, or neurology. The studies collected in this review concern new therapeutic and diagnostic procedures in humans and new structures tested on animals. We also performed an analysis of clinical trials, which concerns application of radiolabeled peptides and antibodies that were reported in the clinicaltrials.gov database between 2008 and 2018.



## INTRODUCTION

Peptides are one of the principal element of all known living systems. They are responsible for many biological functions including, but not limited to, neurotransmission, ion-channel regulation, and regulation of cell growth. The special place in the group of amino acid structures is occupied by antibodies, which are characterized by exceptional selectivity and precision of targeting with the ability to determine biological activity. The wide-ranging applications of peptides and antibodies in medicine are well-known. Because of its multifunctionality, common-ness in the human body, and precise targeting to a specific place of bonding in an organism, peptides and antibodies were considered very promising diagnostic and therapeutic agents or carriers of structures that fulfill these roles. Therefore, radiolabeling of peptides and antibodies was the natural direction for improvement of diagnostic techniques and medical procedures.

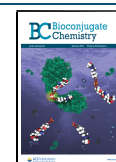
The first radiolabeled peptide used in humans was the somatostatin analogue  $^{123}\text{I}$ -204-090 developed by Krenning et al. in 1989,<sup>1,2</sup> and the first radiolabeled peptide approved by US Food and Drug Administration (FDA) was  $^{111}\text{In}$ -DTPA-octreotide ( $^{111}\text{In}$ -pentetreotide,  $^{111}\text{In}$ -DTPA-octreotide, OctreoScan). OctreoScan has been used in the diagnosis of neuroendocrine tumors since its approval in 1994. The next diagnostic radiolabeled peptide compound approved by the FDA was  $^{111}\text{In}$ -capromab pendetide (ProstaScint) in 1996. It is an  $^{111}\text{In}$  radiolabeled murine monoclonal antibody (7E11-C5.3) with Prostate Specific Membrane Antigen (PSMA) affinity, and it was used in prostate cancer patients with a high risk of pelvic lymph node metastases. ProstaScint was the first

approved agent for use in radioimmunoscintigraphy as well as a key milestone in the development of radioimmunotherapy (RIT). The FDA first approved small synthetic radiolabeled peptides for use in receptor imaging in 1997— $^{99\text{m}}\text{Tc}$ -Apcitide ( $^{99\text{m}}\text{Tc}$ -P280, AcuTect). AcuTect is a small technetium- $^{99\text{m}}\text{Tc}$ -labeled peptide composed of two identical cyclic peptide monomers.<sup>3</sup> The compound binds with high affinity to the  $\text{GPII}_b/\text{III}_a$  receptor on activated platelets, which in turn provide information about localization of thrombi anywhere in the body.<sup>4</sup> Therefore, AcuTect is used for scintigraphic imaging of acute venous thrombosis in the lower extremities of patients with symptoms of acute venous thrombosis. After 2000, the European Medicines Agency (EMA) approved the next radioimmunodiagnostic agent as well as the first radioimmunotherapeutic compound.  $^{99\text{m}}\text{Tc}$ -Besilesomab (Scintimun) is a murine anti-granulocyte antibody used for radionuclide imaging for determining the location of inflammation/infections in the peripheral bone of adults with suspected osteomyelitis.  $^{90}\text{Y}$ -Ibritumomab Tiuxetan (Zevalin) is a murine  $\text{IgG}_1$  antibody used in RIT of adult patients with rituximab relapsed or refractory CD20+ follicular B-cell in non-Hodgkin's lymphoma. The National Center For Nuclear Research POLATOM achieved in 2014 a local Polish approval

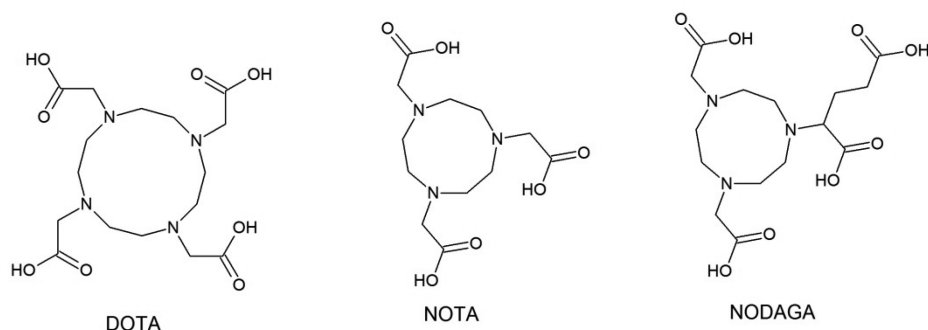
Received: November 11, 2020

Revised: December 2, 2020

Published: December 16, 2020



## Cyclic bifunctional chelators



## Acyclic multidentate bifunctional chelators

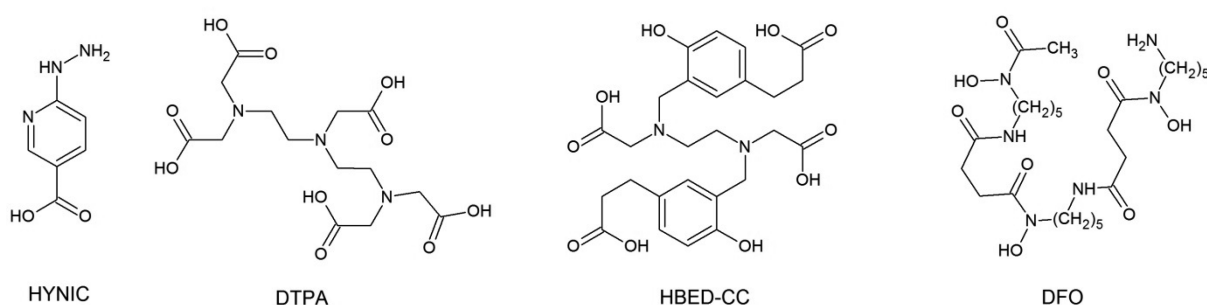


**Figure 1.** Basic structures of the most commonly BFCs used to radiolabeling peptides.

of diagnostic usage their  $^{99m}\text{Tc}$ -Human Immunoglobulin ( $^{99m}\text{Tc}$ -HIG, TechImmuna) only in Poland. This agent is used to detect the location of inflammatory lesions and in semi-quantitative evaluations of inflammatory activity, particularly in the case of rheumatoid arthritis. In the past 3 years, the EMA has approved one diagnostic and one therapeutic radiolabeled somatostatin analogue. POLATOM— $^{99m}\text{Tc}$ -HYNIC-octreotide ( $^{99m}\text{Tc}$ -HYNIC-[D-Phe<sup>1</sup>, Tyr<sup>3</sup>-octreotide]TFA, Tekreotydy)—has been nationally approved in 17 European countries in 2018. It is used in diagnosis and supports the therapy of tumors which overexpress somatostatin receptors as in the case of gastroenteropancreatic neuroendocrine tumors (GEP-NET). Another GEP-NET diagnostic agent was approved in 2016. It was  $^{68}\text{Ga}$ -edotreotide ( $^{68}\text{Ga}$ -DOTA<sup>0</sup>-Phy<sup>1</sup>-Tyr<sup>3</sup>-octreotide,  $^{68}\text{Ga}$ -DOTA-TOC, SomaKit) and is the only approved radiolabeled peptide PET agent in Europe today. The newest therapeutic agent approved by both the FDA and EMA is  $^{177}\text{Lu}$ -oxodotreotide ( $^{177}\text{Lu}$ -DOTA-Tyr<sup>3</sup>-octreotate,  $^{177}\text{Lu}$ -DOTA-TATE, Lutathera). It is used in the therapy of well differentiated neuroendocrine tumors.

**Peptides.** Radiolabeled peptides used in medicine are often modified variants of naturally occurring peptides, because the natural peptides are sensitive to peptidases, which rapidly break them down in blood and other tissues. Nowadays, it is possible to apply two main targeting strategies: peptide–receptor radionuclide therapy (PRRT), peptide–receptor scintigraphy (PRS), radioimmunodiagnosis (RII), and radioimmunotherapy (RIT). The first strategy is based on overexpression of various receptors in human cancer cells, which are attractive targets for imaging and therapy. Particularly interesting targets are somatostatin receptors (SSTRs), gastrin-release peptide receptors (GRPRs),  $\alpha_v\beta_3$  integrin receptors, chemokine

receptors 4 (CXCR4), or glucagon-like peptide 1 (GLP-1) receptors. A multiplicity of targets implies that the PRRT/PRS strategy has a wide spectrum of applications.<sup>5</sup> The second strategy is based on stable *in vivo* monoclonal antibodies (Mabs), or fragments of Mabs as ligands.<sup>6,7</sup>

**Methods of Labeling.** All ligands listed above require the addition of a radionuclide to achieve therapeutic or diagnostic goals. The labeling of peptides can be performed by direct labeling, addition of a prosthetic group, or with bifunctional chelators (BFCs). Direct labeling is the method used to label proteins without using intermediates such as BFCs. It can also be reduced to a one-step labeling protocol, which is an advantage for development of radiopharmaceutical kits and for short-lived radionuclide labeling. An example of this procedure is one-step direct  $^{18}\text{F}$  labeling by displacing a nitro group in an arene that is activated toward nucleophilic aromatic substitution by an ortho trifluoromethyl group.<sup>8</sup> Direct labeling technique nowadays involves mostly radioiodination and in some cases technetium-labeling.<sup>9,10</sup> Technetium direct labeling requires a specific structure of labeled agent coordination sphere, for example, with thiol groups, and reducing agents like phosphines.<sup>11</sup> The disadvantage of this method is that it necessitates a specific protocol for each radioligand as well as difficulty of developing accurate protocols to obtain highly specific products from each applied radionuclides.

Prosthetic groups are small molecules able to bind with radionuclides in one site of the structure, and simultaneously with a peptide at a second site. Radiolabeling peptides by using prosthetic groups is usually a two-step protocol—incorporation of the radionuclide in the prosthetic group structure, followed by binding the prosthetic group to peptide. Each step can be performed according to various methods. A review

article published by Wilbur<sup>12</sup> provides an excellent overview of methods for labeling proteins by radiohalogens. Prosthetic groups allow us to label various peptides, because of the occurrence of multiple reactive functional groups incorporated into amino acid structures. Alcohols, amines, carboxylic acids, and thiols may be paired with the reactive site of a prosthetic group conjugated with a radionuclide to achieve the complete radiolabeled peptide.<sup>13–15</sup> A very effective method of <sup>18</sup>F radiolabeling peptides by using prosthetic groups is the automated “fluorination on the Sep-Pak” method. This method was used in production 6-<sup>18</sup>F Fluoronicotinic acid *N*-hydroxysuccinimide ester (6-[<sup>18</sup>F]SFPy) and then radiolabeling T140 peptide–CXCR4 PET imaging ligand.<sup>16</sup> Another possible method for binding the prosthetic group to a peptide is modification of the peptide to bear unnatural bioorthogonal functional groups like an azide and then by using “click” chemistry to achieve the radiolabeled biomolecule.<sup>17,18</sup> Tolmachev et al. presented a large number of methods for binding prosthetic groups carrying various radionuclides to peptides in their review article.<sup>9</sup>

Despite many advantages, direct labeling and prosthetic groups have limits. These methods of labeling are the most suitable for diagnostic and therapeutic radiohalogens or <sup>11</sup>C, given the reactivity of these nuclides. Radiometals, including <sup>99m</sup>Tc, <sup>68</sup>Ga, <sup>64</sup>Cu, <sup>177</sup>Lu, <sup>111</sup>In, or <sup>90</sup>Y, require BFCs to obtain the best conjugation of radionuclides with peptides. The bifunctional nature of the chelators means that they are capable of coordinating a metal ion and can also be attached to the peptide. Pendant labeling is the most commonly used method of labeling peptides in the present day. There are two main types of BFCs—cyclic BFCs and acyclic multidentate BFCs (Figure 1). 1,4,7,10-Tetraazacyclododecane-1,4,7,10-tetraacetic acid (DOTA), 1,4,7-triazacyclononane-1,4,7-triacetic acid (NOTA), and 2-[4,7-bis(carboxymethyl)-1,4,7-triazonan-1-yl]pentanedioic acid (NODAGA) are widely used cyclic BFCs to coordinate <sup>111</sup>In, <sup>67/68</sup>Ga, <sup>64</sup>Cu, and <sup>99m</sup>Tc, among others. Moreover, the most successful <sup>18</sup>F labeling strategy was developed by McBride et al., which involves using an aluminum-[<sup>18</sup>F]fluoride NOTA derivatives chelator system.<sup>19</sup> Cyclic BFCs are particularly interesting for scientists and medical practitioners because of their universal usage. Peptides conjugated with cyclic BFC can be labeled by various radionuclides which, depending on the applied radionuclide, can provide structures used for therapeutic or diagnostic purposes. This allows for use of the same peptide compound in various imaging technique. Acyclic BFCs are less common than cyclic BFCs, but are still developed due to their selective high affinity for individual radionuclides and their ability to conjugate metal ions at room temperature, which is impossible when using only cyclic BFCs.<sup>20,21</sup> *N,N'*-Bis[2-hydroxy-5-(carboxyethyl)benzyl]ethylenediamine-*N,N'*-diacetic acid (HBED-CC) has high affinity to Ga<sup>3+</sup> ions.<sup>22</sup> 1,1,4,7,7-Diethylene triaminopentaacetic acid (DTPA) is applicable in <sup>111</sup>In, <sup>90</sup>Y, and <sup>68</sup>Ga radiolabeling of thermosensitive peptides.<sup>20,23–25</sup> Desferoxamine (1-amino-6,17-dihydroxy-7,10,18,21-tetraoxo-27-(*N*-acetylhydroxylamino)-6,11,17,22-tetraazaeptaicosane, DFO) is originally an iron and aluminum chelator, but DFO also complexes Ga<sup>3+</sup> ions rapidly<sup>23</sup> and is one of the best <sup>89</sup>Zr carriers for labeling intact Mabs.<sup>26</sup> 2-Hydrazinonicotinic acid (HYNIC) is a well-known and commonly used <sup>99m</sup>Tc carrier.<sup>27,28</sup> BFCs also have some disadvantages. BFC moieties are generally bulky, and as a result are usually located far away from the binding region of

peptides to avoid steric interactions. BFCs are often placed at the *N*- or *C*-terminus of the peptide. Often, additional spacers are used, which increases the molecular weight of whole structure, an adverse fact especially for small peptides.<sup>29</sup> The labeling can influence charge or lipophilicity of the compound, which in turn may change its biodistribution or excretion, particularly for small ligands. The right selection of labeling method is therefore crucial to obtain appropriate resolution of images, concentration in tumors cells, and excretion methods with efficient clearance.<sup>30</sup>

**Radionuclides.** The type of radionuclide used is the third most important property of radiolabeled peptides. The radionuclides can be used for therapeutic or diagnostic purposes, and a small group of radionuclides may be used for both. Examples of these include theranostic radionuclides, <sup>177</sup>Lu, <sup>67</sup>Cu, and <sup>111</sup>In.<sup>31</sup> Diagnostic radionuclides are used in molecular imaging modalities applied in nuclear medicine: SPECT and PET. Because of different mechanisms of action, each imaging method requires different radionuclides. Both modalities require the emission of photons in the form of radiation, which can be detected and processed into an image. However, this radiation has to originate from positron annihilation for PET imaging, while SPECT imaging require radionuclides that emit a direct gamma array with approximately 100–250 keV gamma energy, which is detected by scintillation detectors. Lower gamma energy produces too much scatter, but greater gamma energy than this range results in poor imaging quality due to difficulty in collimating the rays.<sup>25</sup> SPECT has an additional advantage in that it is possible to simultaneously image multiple radiometals emitting  $\gamma$  rays with different energies.<sup>32</sup> PET imaging requires radionuclides which emit positrons. A single positron is formed during  $\beta^+$  decay. The annihilation of positrons is pivotal for this modality of imaging, because this process generate two photons, each of 511 keV, in opposite directions. This phenomenon allows for determination of the location of annihilation in three dimensions by calculating the time difference between both photons reaching the detectors. Additional simultaneously emitted  $\gamma$  rays from radionuclides are also filtrated, because only two precisely opposed rays—an interesting result of annihilation are used to image generation. The mean free path of a positron is one of the most important properties of radionuclides used in PET imaging. Short mean free paths provide increased image resolution. Mean free energy emitted from positron emission can influence on resolution; therefore, radionuclides with small positron energy produce higher resolution. In addition, mean free energy affects the surrounding tissues.<sup>21</sup> The half-life of radionuclides is the most significant property to be understood, independent from the radionuclide's purpose. Half-lives should be long enough to allow the peptide to accumulate in the target and clear from other compartments. Short-lived radionuclides are usually used in imaging especially because using small peptides tends to show fast biodistribution and clearance. Longer-lived radionuclides are used in imaging with peptides with long biodistribution and clearance and in therapy.<sup>9</sup> The most common in radionuclides are shown in Table 1.

## ■ NEW REPORTS OF RADIOLABELED AMINO ACID BASED MOLECULES USED IN NUCLEAR MEDICINE

**SSTR.** Somatostatin receptors (SSTR) are neuroreceptors at the cell membrane, which may be used for diagnostic and



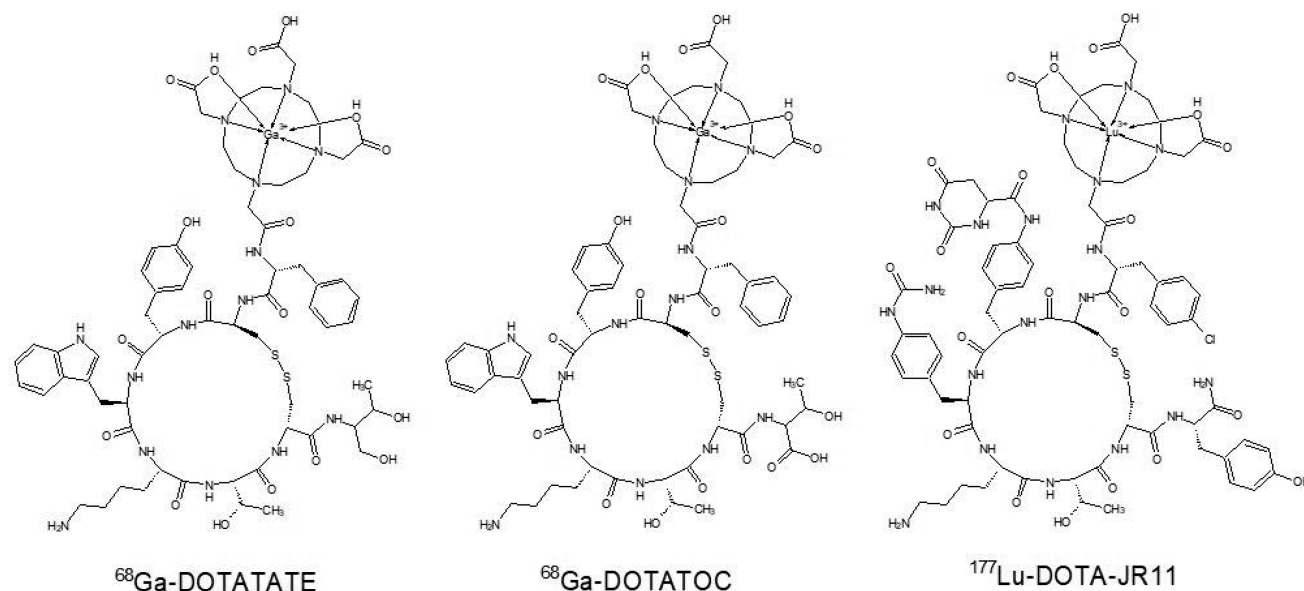
**Table 1.** Physical Characterization of Radionuclides Used in Radiolabeling Peptides<sup>21,33–36</sup>

nuclide	half-life	decay mode	mean free path (mm)	mean free energy (keV)	gamma energy (keV)
PET imaging isotopes					
<sup>18</sup> F	109.8 min	$\beta^+$ (97%)	0.6	250	-
<sup>76</sup> Br	16.2 h	$\beta^+$ (54%)	1.2	633.9	-
EC (46%)					
<sup>68</sup> Ga	67.7 min	$\beta^+$ (87%)	3.5	844	-
<sup>64</sup> Cu	12.7 h	$\beta^+$ (17%)	0.7	278	-
$\beta^-$ (39%)					
EC (44%)					
<sup>11</sup> C	20.4 min	$\beta^+$ (100%)	1.2	386	-
<sup>89</sup> Zr	3.3 d	$\beta^+$ (23%)	1.3	396	-
EC (77%)					
<sup>124</sup> I	4.2 d	$\beta^+$ (23%)	0.9	819	603
EC (77%)					
Radiotherapeutic isotopes					
<sup>90</sup> Y	64 h	$\beta^-$ (100%)	2.5	935	-
<sup>131</sup> I	8 d	$\beta^-$ (100%)	-	970.8	-
<sup>177</sup> Lu	6.7 d	$\beta^-$ (79%)	0.7	130	208 and 113
<sup>211</sup> At	7.2 h	$\alpha$ (100%)	0.06	6790	-
<sup>225</sup> Ac	10 d	$\alpha$ (100%)	0.06	6830	-
Gamma imaging isotopes					
<sup>111</sup> In	2.8 d	EC (100%)	-	-	171 and 245
<sup>123</sup> I	13.2 h	EC (97%)	-	-	159
<sup>99m</sup> Tc	6 h	EC (98%)	-	-	140

therapeutic purposes. Their occurrence is common in GEP NETs. This fact have been used for more than 20 years for precise GEP NETs imaging and therapy by application as SSTR analogues.<sup>37</sup> A cohort study of North American patients with metastatic well-differentated NETs indicate that PRRT with SSTR analogues resulted long overall survival (over 40 months from first PRRT) and time to progression (the median was 23.9 months).<sup>38</sup>

Recent studies in human models are often focused on optimization and individualization of therapy. Velikyan et al. performed a pilot study to discover the impact of peptide mass on the binding of <sup>68</sup>Ga-DOTATOC (Figure 2) to neuroendocrine tumor somatostatin receptors in 9 patients with GEP NETs in 2010. The peptide mass was considered as the peptide mass of SSTR analogue required to occupy the natural SSTRs in the body during the imaging process to obtain the best image contrast and higher tumor-to-normal tissue ratio. They were looking for the optimal unlabeled peptide mass administrated a short time before the tracer. Their study demonstrated that individual patient uptake of radiolabeled ligand in tumor and normal organs exhibited peptide mass dose dependence.<sup>39</sup> Hardiansyah et al. investigated PET-based treatment planning by using the physiologically based pharmacokinetic (PBPK) model with mathematical patient phantoms and Bayesian parameters or dynamic PET. Their aim was to investigate the accuracy of predicting the time-integrated activity coefficients (TIACs). TIACs are the accumulated activities in source organs per administered activity and are also called residence times. They proved that <sup>68</sup>Ga-DOTATATE PET measurements could be used to predict the therapeutic biodistribution of <sup>90</sup>Y-DOTATATE with acceptable accuracy if all available information is integrated in PBPK.<sup>40–42</sup>

<sup>177</sup>Lu-DOTATATE is also one of the most common compounds applied in recent publications because of recent approval of Lutathera. Researchers report possible side effects, quality of life changes, and effects of the therapy. <sup>177</sup>Lu-DOTATATE as a PRRT agent may induce long-term toxicity to the bone marrow, but a study performed on 274 GEP-NET

**Figure 2.** Schemes of SSTR analogues applied in new PRRT and PRS strategies.

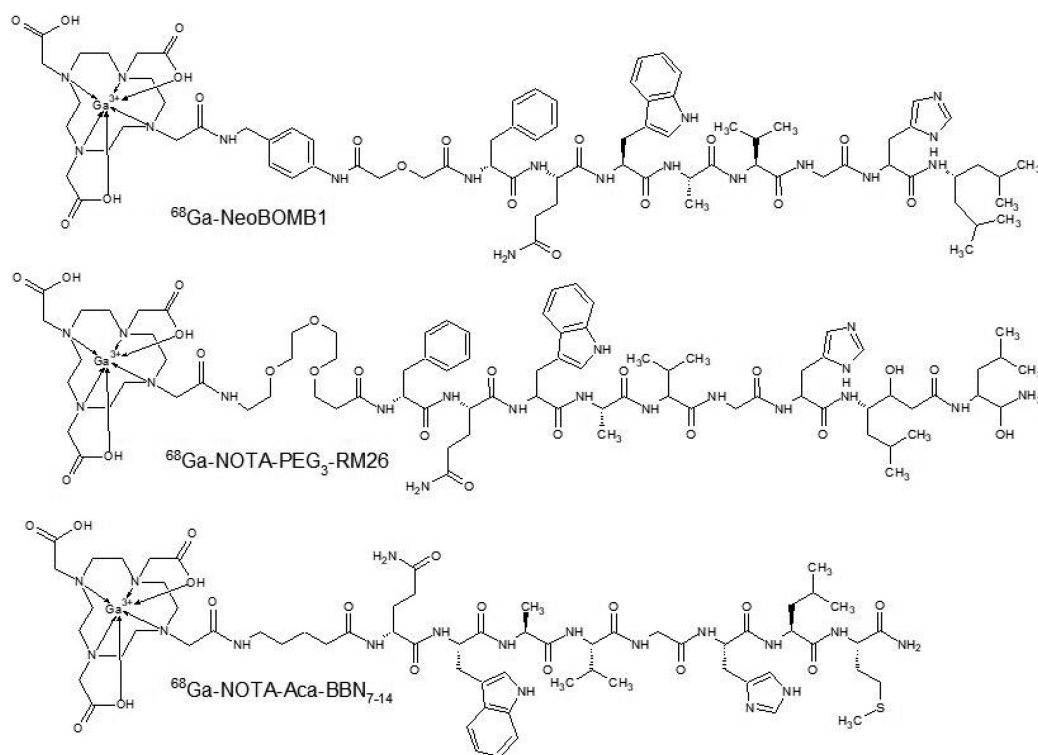


**Figure 3.** Schemes of GRPR analogues applied in new PRS strategies.

patients confirms that  $^{177}\text{Lu}$ -DOTATATE therapy has no risk factors for developing persistent hematological dysfunction in GEP-NET patients.<sup>43</sup> Furthermore, two independent studies confirm that  $^{177}\text{Lu}$ -DOTATATE therapy increases the quality of life of GEP-NET patients.<sup>44,45</sup> Hervas et al. performed a summary of experience with  $^{177}\text{Lu}$ -DOTATATE. They evaluated the biochemical response, imaging methods, toxicity, and quality of life of treatment for 7 patients with metastatic NET. Results of this study indicate the efficacy and safety of  $^{177}\text{Lu}$ -DOTATATE.<sup>45</sup> Ashley et al. reported a case in which they applied a  $^{177}\text{Lu}$ -DOTATATE neoadjuvant therapy before multivisceral transplantation in patients with metastatic small intestinal neuroendocrine neoplasm. The result of their therapy protocol is the lack of biochemical and radiological disease recurrence over 4 years after the intervention.<sup>46</sup>  $^{177}\text{Lu}$ -DOTATATE was also used to develop a PBPK model of  $^{177}\text{Lu}$  peptide therapy of patients with NET. It can be used for accurate calculation of biodistribution and absorbed doses of patients during individual planning of therapy.<sup>45</sup> Zemczak et al. studied the therapeutic effect of a mixture of  $^{177}\text{Lu}$  and  $^{90}\text{Y}$  DOTATATE. 75 patients with histopathologically proven NET G1 and G2 and after  $^{18}\text{F}$ -FDG PET/CT imaging were included in the study. Results of the therapy were in line with similar procedures with single isotope  $^{177}\text{Lu}$  DOTATATE, but they discovered that  $^{18}\text{F}$ -FDG positive patients have higher risk of progression in the two year follow-up.<sup>47</sup> A similar study was performed by Kunikowska et al. They included 103 patients with NET G1/G2 and also applied  $^{177}\text{Lu}/^{90}\text{Y}$  DOTATATE treatment. Their results are also very promising. Moreover, the study proved low hematological and renal toxicity.<sup>48</sup>

Imaging techniques with radiolabeled SSTR ligands have also improved. Nowadays, medicine uses PET-MRI and PET-CT scanners to image tumors and metastasis by using  $\beta^+$  decay-type radionuclides, where PET-CT is a clinical routine

in practice. Nevertheless, PET-MRI is able to obtain superior soft-tissue contrast and functional information. Furthermore, the dynamic contrast enhanced imaging with hepatocellular contrast agents is able to detect liver metastases. Therefore, whole-body PET-CT and PET-MRI imaging with  $^{68}\text{Ga}$ -DOTANOC was compared in patients with well-differentiated neuroendocrine tumors. The results indicate that PET-MRI is comparable with PET-CT. In addition, the application of the gadoxetate contrast protocol allows for detection of the liver metastasis, but the PET-CT technique was more effective in detecting lung lesions.<sup>49</sup>

Researchers focused on SSTRs agonists first. The most common radiolabeled structures as DOTATOC or DOTATATE are agonists, but nowadays the new points of interest are SSTR antagonists. Despite the internalization of the radionuclide into tumor cells, which is achievable by application of SSTR agonists, antagonists are capable of interacting with more binding sites. This fact may be more important than internalization of SSTR agonists.<sup>50–52</sup> Recent studies report on the effectiveness of use OPS201 (DOTA-JR11). JR11 is SSTR antagonist. Conjunction with DOTA allows for radiolabeling with for example  $^{177}\text{Lu}$ ,  $^{90}\text{Y}$ , and  $^{111}\text{In}$ . Nicolas et al. investigated OPS201 labeled with  $^{177}\text{Lu}$ ,  $^{90}\text{Y}$ , and  $^{111}\text{In}$  and compared it with  $^{177}\text{Lu}$ -DOTATATE on cell lines and a mouse model. Their results indicate that  $^{177}\text{Lu}$ -OPS201 exhibits a higher tumor uptake, longer tumor residence time, and improved tumor-to-kidney dose ratio than  $^{177}\text{Lu}$ -DOTATATE or  $^{90}\text{Y}$ -OPS201. Moreover, they confirmed that  $^{111}\text{In}$  should not be used as a surrogate for  $^{90}\text{Y}$  radiolabeled OPS201. Recommendations for nephroprotective agents which may be used in PRRT with  $^{177}\text{Lu}$ -OPS201 (Figure 2) are also a valuable conclusion of this study.<sup>53</sup> A similar study was performed by Dalm et al. They focused on usage of  $^{111}\text{In}$ -

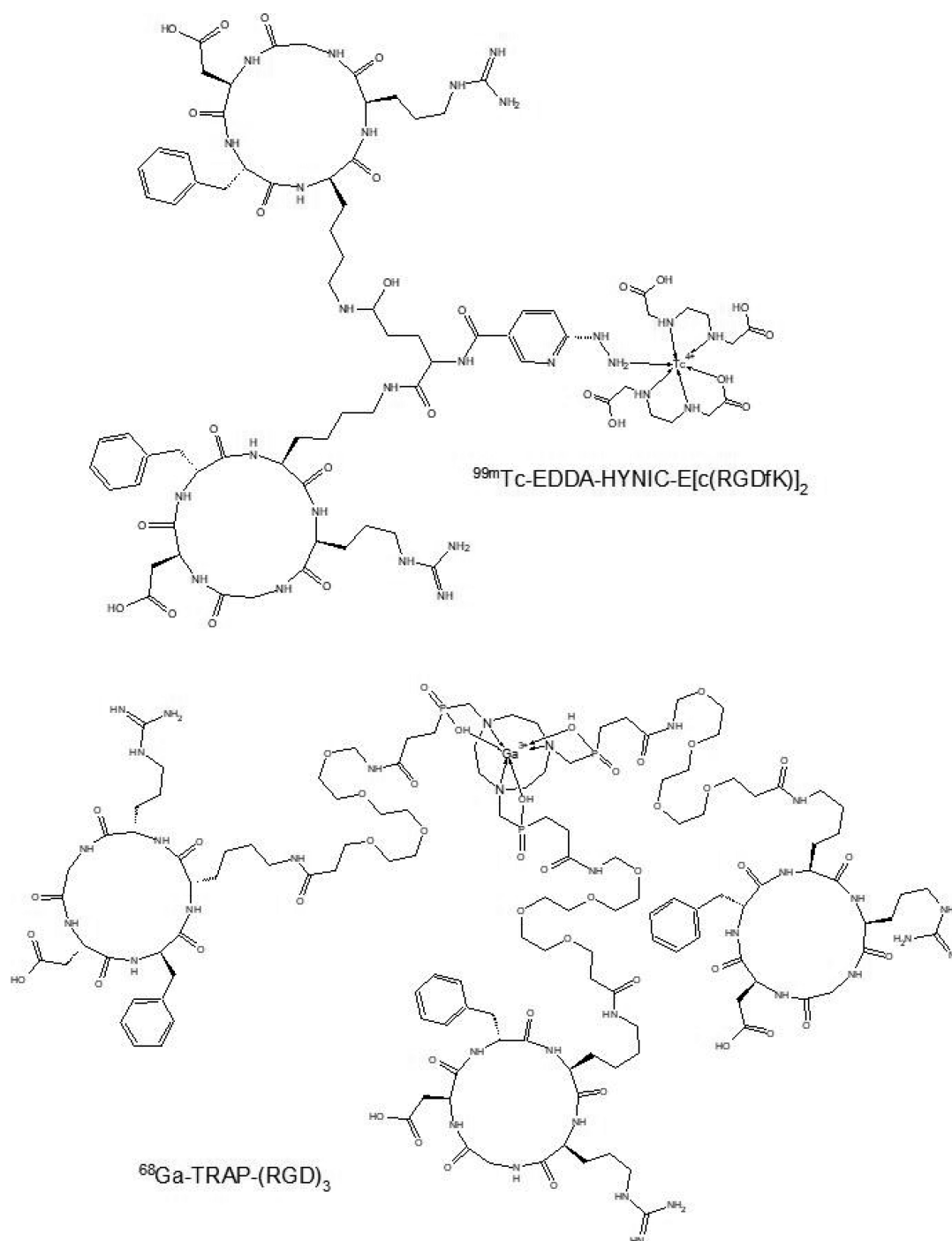


**Figure 4.** Schemes of RGD derivatives applied in new PRS strategies.

OPS201 in breast cancer imaging. This study also confirmed that OPS201 is a promising candidate for usage in medicine.<sup>54</sup>

**GRPR.** The gastrin-releasing peptide receptor (GRPR) is one of the bombesin receptors and a G-protein coupled receptor. Overexpression of GRPR was found in small cell lung cancer for the first time. Scientist found it later in many different tumors including breast, pancreatic, or prostate cancer.<sup>55,56</sup> Morgat et al. studied the GRPR overexpression in breast cancer patients. They found the GRPR overexpression in 75.8% of 1432 tumors studied, of which 83.2% were estrogen receptor (ER) positive. Besides the association of GRPR overexpression and ER positivity, scientists also

found GRPR expression in metastatic lymph nodes in 94.6% of cases with overexpressed GRPR tumor. Results led to conclusion that GRPR targeting is good strategy for imaging and treatment in patients with ER positive breast cancer.<sup>57</sup> Recent studies report GRPR antagonist research in human models. Despite the internalization in cancer cells, GRPR agonists may cause undesirable effects after induced GRPR activation.<sup>58</sup> Therefore, novel GRPR antagonist peptide radiotracers are developed. Berthold et al. developed Neo-BOMB1 and conjugated it with  $^{177}\text{Lu}$ ,  $^{68}\text{Ga}$ , and  $^{111}\text{In}$ . They performed a biologic profile resulting in all radiolabeled NeoBOMB1 conjugating to GRPR-expressing cells as well as

mouse models, and first prostate cancer lesion visualization in human patients using  $^{68}\text{Ga}$ -NeoBOMB1 and PET/CT. Results indicate that NeoBOMB1 binds to GRPR with high affinity and with low internalization. Mouse model study provided information about good metabolic stability in peripheral mouse blood, high and specific uptake, and clearing from background via the kidneys. PET/CT scans of two patients showed that using  $^{68}\text{Ga}$ -NeoBOMB1 provides high-contrast imaging of pathologic lesions in humans. Scientists intend to continue research to investigate theranostic value of NeoBOMB1 in nuclear oncology.<sup>59</sup>

NeoBOMB1 was investigated also on animal models. Two independent teams performed studies about the theranostic use of  $^{68/67}\text{Ga}$ -NeoBOMB1 in breast and prostate cancer. Kaloudi et al. investigated  $^{68}\text{Ga}$ -NeoBOMB1 and  $^{67}\text{Ga}$ -NeoBOMB1 profiles on GRPR expressing T-47D cells as well as mice bearing human T-47D xenografts.  $^{67}\text{Ga}$ -NeoBOMB1 showed high affinity for GRPR on T-47D cell membranes with poor internalization. Mice models provided biodistribution data. >90% intact of dose was detected in mice peripheral blood at 30 min post-injection.  $^{67}\text{Ga}$ -NeoBOMB1 localized tumor in mice bearing T-47D xenografts. Increasing the dose of NeoBOMB1 to 200 pmol reduced the unfavorably high pancreatic uptake without change in tumor uptake.<sup>60</sup> Dalm et al. investigated the biodistribution of  $^{68}\text{Ga}$ -NeoBOMB1 and  $^{177}\text{Lu}$ -NeoBOMB1 on PC-3 xenograft BALB/c mice. They obtained similar results, indicating a good pharmacokinetic profile of NeoBOMB1. The improvement of the tumor/pancreas uptake ratio was also observed by increasing the dose of peptide.<sup>61</sup> Another  $^{68}\text{Ga}$  labeled GRPR antagonist RM26 (Figure 3) was compared with GRPR agonist BBN<sub>7-14</sub> by using PC-3 cells and PC-3 tumor xenografted mice. Both compounds indicated similar affinity to GRPR, but biodistribution data obtained from in vivo studies show a better profile for RM26. BBN<sub>7-14</sub> demonstrated rapid elimination after injection, high background signal, and high level of degradation in mice serum in comparison to RM26. Antagonists offer improved tumor to organ ratios as well as better image results due to lower accumulation in the pancreas and intestines.<sup>62</sup> Improved profiles of GRPR antagonists were also confirmed by Liolios et al. They developed four  $^{68}\text{Ga}$  labeled analogues of bombesin connected with HBED-CC chelator—two agonists and two antagonists. Due to the presence of two connectable carboxylic moieties in the structure of HBED-CC, one of the antagonist structures was a homodimer. All compounds were investigated by using PC-3 and T-47D cell lines to obtain information about cell-bound radioactivity. The best results were obtained for the homodimeric antagonist structure in both cell lines. In vivo assays with PC-3 tumor bearing mice and  $\mu\text{PET}$  imaging provided information about better quality imaging by using antagonist structures. Despite exceptionally good results with respect to cell bonding and imaging quality of dimeric antagonists, the monomeric structure had a superior pharmacokinetic profile as a result of lower AUC values for nontarget organs and blood relative to the dimeric form.<sup>63</sup>

**$\alpha_v\beta_3$  Integrin Receptors.**  $\alpha_v\beta_3$  and  $\alpha_v\beta_5$  integrins are used as indicators in breast cancer as they signal cell growth, including malignancy, metastasis, and cancer induced angiogenesis. They are overexpressed in tumor and endothelial cells of breast cancer.<sup>64,65</sup> Small peptide sequence Arg-Gly-Asp (RGD) has been reported as a structure that is recognized by integrins. Therefore, radiolabeled structures with an RGD core

were used as radiopharmaceuticals with high affinity and selectivity for the  $\alpha_v\beta_3$  and  $\alpha_v\beta_5$  integrins.<sup>66</sup> The research performed on the RGD sequence has provided many new structures such as dimeric compounds, that offer much greater affinity to  $\alpha_v\beta_3$  integrins than the monomer. Ortiz et al. developed a biokinetic model for  $^{99\text{m}}\text{Tc}$ -EDDA/HYNIC-E-[c(RGDfK)]<sub>2</sub> (Figure 4) from a lyophilized formulation kit. Ethylenediamine-*N,N'*-diacetic acid (EDDA) was used as a coligand in radiolabeling of HYNIC-peptides to complete the technetium coordination sphere. In addition, the scientists chose EDDA as a coligand because of its hydrophilic properties that improved renal excretion and allowed it to combine in lyophilized formulation. Scientists obtained  $96 \pm 2\%$  purity after labeling, and biodistribution studies in mice showed renal and hepatobiliary excretion.  $^{99\text{m}}\text{Tc}$ -EDDA/HYNIC-E-[c(RGDfK)]<sub>2</sub> has high affinity and showed highly specific uptake to MCF7, T47-D, and MDA-MB-231 cell lines. The imaging in three breast cancer patients localized lesions with high contrast. In addition, ten healthy patients took part in this study. None of patients reported any adverse reactions after  $^{99\text{m}}\text{Tc}$ -EDDA/HYNIC-E-[c(RGDfK)]<sub>2</sub> administration. It was observed that thyroid and kidneys were the organs which received the highest absorbed dose, but these amount of absorbed doses were comparable to different  $^{99\text{m}}\text{Tc}$  radiopharmaceutical studies.<sup>67,68</sup> Zhang et al. performed a study in which they evaluated imaging of breast cancer and metastasis with a dual targeting tracer  $^{68}\text{Ga}$ -BBN-RGD PET/CT. Twenty-two female patients with suspected breast cancer who underwent radical mastectomy were sampled to take part in this study.  $^{68}\text{Ga}$ -BBN-RGD showed high tumor to organ ratios, which in turn provided high contrast in PET/CT image. According to Morgat et al., higher maximum standardized uptake values were observed in patients with ER-positive tumors because of higher overexpression of GRPR in tumor cells. In addition,  $^{68}\text{Ga}$ -BBN-RGD was compared with  $^{68}\text{Ga}$ -BBN. Results of this comparison indicated that dual targeting tracer localized more pathological lesions than  $^{68}\text{Ga}$ -BBN.<sup>69</sup> Kazmierczak et al. investigated the  $^{68}\text{Ga}$ -TRAP-(RGD)<sub>3</sub> (Figure 4) for in vivo monitoring of a  $\alpha_v\beta_3$  integrin expression as a biomarker of anti-angiogenic therapy effects by using PET/CT. They used 25 mice bearing MDA-MB-231 xenografts which were divided into two cohorts. The first cohort was subject to imaging tests and the second to immunohistochemistry tests. Either anti VEGF antibody bevacizumab or a placebo was administrated for a week in the experimental protocol. Imaging with  $^{68}\text{Ga}$ -TRAP-(RGD)<sub>3</sub> at the beginning and at the end of study allowed for observation of reductions in  $\alpha_v\beta_3$  integrin expression in xenografts. Immunohistochemistry assays confirmed that bevacizumab therapy caused reduction of  $\alpha_v\beta_3$  integrin expression, microvascular density proliferation, and increase of tumor cell apoptosis. Therefore,  $^{68}\text{Ga}$ -TRAP-(RGD)<sub>3</sub>PET/CT allows for monitoring of anti-angiogenic therapeutic effects which scientists will continue to explore.<sup>70</sup>

**GLP-1 Receptors.** Glucagon-like peptide 1 (GLP-1) is an incretin secreted from intestinal L cells. It is able to activate GLP-1 receptors which play a significant role in glucose metabolism. Scientists also reported positive effects from activation of GLP-1 receptors on decrease of pancreatic  $\beta$ -cell apoptosis and even increased differentiation of  $\beta$ -cell precursor cells in the pancreas.<sup>71,72</sup> Overexpression of GLP-1 receptors was found in a number of cancers such as gastrinomas or insulinomas. GLP-1 receptors in insulinomas are expressed in



the highest incidence and density among any other peptide receptors in this type of tumor; therefore, GLP-1 receptors offer great potential as a diagnostic target. Azad et al. investigated the GLP-1 receptors through optical and PET imaging. They synthesized and evaluated GLP-1 analogues with a DOTA bifunctional chelator and one analogue combined with fluorescein. Two of these analogues were radiolabeled by  $^{68}\text{Ga}$  and administered to normal CD1 and C57BL/6 mice for biodistribution evaluation and Balb/c<sup>nu/nu</sup> mice harboring insulinomas for imaging tests. The pancreatic uptake in CD1/C57BL/6 mice observed after 30 min post injection was low and stable. Imaging tests provide clearly visualized tumor after 90 min post injection. Scientists compared results of radiolabeled GLP-1 analogues with radiolabeled exendin-3 and exendin-4. Radiolabeled GLP-1 analogues indicated faster overall clearance rate than exendin-3 and exendin-4, but also a lower tumor uptake.<sup>73</sup> Bauman et al. had a similar goal in their study, but they investigated  $^{68}\text{Ga}$  and  $^{89}\text{Zr}$  radiolabeled exendin-4. Exendin-3 and exendin-4 are reptilian agonists of GLP-1 receptors. Exendin-4 is especially interesting, because it is not degraded by dipeptidylpeptidase 4, and exhibits a 10-fold-increase in affinity toward human GLP-1 receptor. Because of the low spatial resolution of SPECT images obtained by  $^{111}\text{In}$  radiolabeled exendin-4 reported in earlier studies,<sup>74,75</sup> Bauman et al. developed an exendin-4 derivative conjugated to desferoxamine (DFO). Utilization of DFO allowed for radiolabeling of one derivative by both  $^{68}\text{Ga}$  and  $^{89}\text{Zr}$  radionuclides. PET imaging results indicate that [ $^{40}\text{Lys}(\text{AHX-DFO-}^{68}\text{Ga})\text{NH}_2$ ]exendin-4 developed by Bauman et al. on nude mice bearing RIN-m5F xenografts is a promising candidate for clinical translation. A comparison of results with [ $^{40}\text{Lys}(\text{AHX-DTPA-}^{111}\text{In})\text{NH}_2$ ]exendin-4 showed that novel radiotracers exhibit comparable or even superior targeting of GLP-1 receptors.<sup>76</sup> Antwi et al. used  $^{68}\text{Ga}$ -DOTA-exendin-4 to localize benign insulinoma lesions in 52 human patients by PET/CT. They compared imaging results with  $^{111}\text{In}$ -DOTA-exendin-4 SPECT/CT and MRI. The highest values of accuracy, impact for surgery planning, and percentage reading agreement were obtained for PET/CT imaging.<sup>77</sup> Parihar et al. reported a case study which used the same radiolabeled tracer on a 31-year-old patient to localize pathological lesions on the pancreas. The patient suffered from gradually increasing lethargy and multiple episodes of dizziness. Biochemical examinations raised suspicions of insulinoma. PET/CT imaging with  $^{68}\text{Ga}$ -DOTA-exendin-4 allowed for identification of localized lesions and surgical intervention. The patient underwent surgical enucleation, after which he experienced an uneventful and complete postoperative recovery.<sup>78</sup>

The GLP-1 receptor is also a target for imaging of  $\beta$  cells of intact pancreatic islets in monitoring type II diabetes or transplanted islets in monitoring type I diabetes therapy. Mikkola et al. performed a study measuring stability, affinity, biodistribution, and PET imaging quality of  $^{64}\text{Cu}$  and  $^{68}\text{Ga}$  labeled [ $^{14}\text{Nle},^{40}\text{Lys}(\text{Ahx-NODAGA})\text{NH}_2$ ]exendin-4 in rats. Results indicate better image properties for  $^{64}\text{Cu}$  labeled tracer, but high radiation doses observed in the kidneys may be the limitation of application of this structure in the future.<sup>79</sup> Li et al. evaluated  $^{68}\text{Ga}$ -DO3A-VS-Cys<sup>40</sup>-exendin-4 as a tracer for imaging human transplanted islets in the mouse liver. They chose the liver as it offers the best target to background contrast. Additional examinations confirmed the number and function of transplanted islets, and the imaging tests provided information about high contrast in images. Biodistribution

tests revealed that the uptake in livers with transplanted islets was 6-fold higher than in the livers of mock transplanted mice. Scientists are working on the application of  $^{68}\text{Ga}$ -DO3A-VS-Cys<sup>40</sup>-exendin-4 in PET quantification of human islet mass and function in clinical applications.<sup>80</sup>

Wang et al. focused on the presence of GLP-1 receptors in the brain, and examined the influences of age on GLP-1 receptors expression using NOTA-MAL-Cys<sup>39</sup>-exendin-4 radiolabeled with aluminum  $^{18}\text{F}$  fluoride and uPET imaging. uPET imaging provided data about the variable uptake of  $^{18}\text{F}$ -AIF-NOTA-MAL-Cys<sup>39</sup>-exendin-4 with respect to regions of the brain. They compared images of nine aged and nine normal rat brains and concluded that the expression of GLP-1 receptors in rat brains decreased with age. Researchers noted the differences in uptake, based on rat ages and regions of brain. They justified this by the fact that variable distribution depended on both brain region as well as and differential expression of GLP-1 receptors in each rat. Therefore, they predicted unique  $^{18}\text{F}$ -AIF-NOTA-MAL-Cys<sup>39</sup>-exendin-4 uptake patterns for different neurological diseases. Biodistribution studies indicated that  $^{18}\text{F}$ -AIF-NOTA-MAL-Cys<sup>39</sup>-exendin-4 is primarily excreted from the renal system due to high uptake in kidneys. The second organ indicating significantly increased higher uptake relative to others was the pancreas. Scientists noted also that this method required further work in part because a small group of rats was used in this study to obtain reliable results, the yield of radiotracer was also not satisfactory, and kidney uptake was too high, which may cause renal damage.<sup>81</sup>

**CXCR4.** The chemokine receptor 4 (CXCR4) is widely expressed throughout the human body G protein-coupled receptor. Together with chemokine CXCL12, which is produced mainly in the bone marrow, lymph nodes, lung, heart, thymus, and liver, CXCR4 forms a CXCL12-CXCR4 signaling axis.<sup>82</sup> This pathway is involved in the homeostasis of the adult hematopoietic system and adequate response of the immune system.<sup>83</sup> CXCR4 has also been found to be involved in a numerous diseases: HIV-1 infection,<sup>84</sup> rheumatoid arthritis,<sup>85</sup> atherosclerosis,<sup>86</sup> chronic inflammation,<sup>87</sup> and even neurodegenerative diseases.<sup>88</sup> In oncology, CXCR4 plays a pivotal role in tumor development and metastasis, which has been proven for breast, prostate, lung, colorectal cancer, or primary brain tumors such as glioblastoma.<sup>83</sup> Therefore, CXCR4 is an attractive target for imaging and therapeutic purposes.

Nowadays, two radiolabeled peptide imaging molecules, which are CXCR4 ligands, were already tested on human patients— $^{68}\text{Ga}$ -Pentixafor and  $^{68}\text{Ga}$ -NOTA-NFB.  $^{68}\text{Ga}$ -Pentixafor is an FC-131 based cyclic pentapeptide radiolabeled with DOTA chelator conjugated with amino acid structure via 4-(aminomethyl) benzoic acid.<sup>89</sup> In 2015, Wester et al. for the first time investigated the effectiveness of the imaging properties of this agent in patients with lymphoproliferative diseases.  $^{68}\text{Ga}$ -Pentixafor bound with high affinity and selectivity to human CXCR4. PET scan with this agent provided images with good specificity and contrast. Dosimetry studies have provided data with even better properties than  $^{68}\text{Ga}$ -DOTATOC or  $^{68}\text{Ga}$ -DOTATATE for absorbed doses in organs.  $^{68}\text{Ga}$ -Pentixafor also showed very good pharmacokinetic profile and fast clearance kinetics.<sup>90</sup> Similar results and conclusions were obtained by Breun et al., who investigated the use of PET/CT  $^{68}\text{Ga}$ -Pentixafor scan in patients with vestibular schwannomas.<sup>91</sup> The second mentioned agent was



$^{68}\text{Ga}$ -NOTA-NFB.  $^{68}\text{Ga}$ -NOTA-NFB is a derivative of 14-amino-acid peptide, CXCR4 inhibitor—T140. Peptide structure was modified by changing the binding site of the disulfide bridge and conjugating NOTA chelator for radionuclide labeling. Wang et al. investigated this agent in healthy volunteers and patients with glioma.  $^{68}\text{Ga}$ -NOTA-NFB was safe and well-tolerated, and it displayed a rapid activity clearance from blood circulation. Imaging studies proved to be more sensitive glioma detecting results than  $^{18}\text{F}$ -FDG PET/CT. Unfortunately, the clearance pattern of  $^{68}\text{Ga}$ -NOTA-NFB exhibited very high splenic and liver uptake, which challenged the application of  $^{68}\text{Ga}$ -NOTA-NFB PET/CT in high contrast clinical imaging of CXCR4 expression.<sup>92</sup> Despite moderate results of  $^{68}\text{Ga}$ -NOTA-NFB, other modifications to the T140 derivatives are under development.<sup>16,93</sup>

There are also other radiolabeled amino acid structures under development that are able to imaging CXCR4. Li et al. reported a  $^{64}\text{Cu}$  radiolabeled modified ubiquitin molecule. Ubiquitin is a small regulatory protein and natural CXCR4 ligand. Li et al. modified ubiquitin structure by addition a C-terminal GGCGG sequence and functionalized the whole structure with trans-cyclooctane (TCO) moiety via thiol-maleimide click reaction. The obtained structure (UbCG4-TCO) was  $^{64}\text{Cu}$ -radiolabeled through TCO/tetrazine-based Diels–Alder click reaction. The obtained molecule was  $^{64}\text{Cu}$ -Cb-1K1P-UBCG4. The molecule was investigated as imaging agent on mice with 4T1 breast cancer xenografts. The results indicate good quality of imaging 4T1 cells with low backgrounds. Dosimetry studies results indicate relatively low accumulation in normal tissues and organs.

CXCR4 is also a good therapeutic and theranostic aim. The therapeutic peptide CXCR4 agent is Pentixafer (3-iodo-D-Tyr<sup>1</sup>-Pentixafer). This Pentixafer derivative was labeled by  $^{177}\text{Lu}$  and investigated on Daudi-lymphoma veering SCID mice and patients with multiple myeloma by Schottelius et al. Tests results on mice and patients indicated very promising CXCR4 targeting characteristics (total cellular tracer uptake is improved compared to  $^{68}\text{Ga}$ -Pentixafer, but internalization at time point  $\geq 15$  min was lower than reference) and suitable pharmacokinetic profile (rapidly cleared from stomach, intestines, and kidneys, but slow excretion from the liver, which can be controlled by coinjection of an excess of unlabeled competitor). The dose-limiting organ for  $^{177}\text{Lu}$ -Pentixafer agent are kidneys.<sup>94</sup> Lau et al. reported a theranostic pair  $^{68}\text{Ga}/^{177}\text{Lu}$ -BL01. BL01 is a modified derivative of LY2510924 (cyclic peptide, CXCR4 inhibitor) by conjugating DOTA chelator with lysine residue at the C terminus of peptide. Because of its structure, BL01 can be radiolabeled by  $^{68}\text{Ga}$  as well as  $^{177}\text{Lu}$ ; therefore, it was a very promising candidate to develop a pair of theranostic agents.  $^{68}\text{Ga}/^{177}\text{Lu}$ -BL01 was investigated on mice bearing Daudi Burkitt's lymphoma xenografts. PET/CT scan shows significant radioactivity in the tumor, liver, kidneys, and bladder. Image contrast was improved at 2 h post injection. Tumor uptake also increased with continued clearance from nontarget tissues. The uptake of  $^{177}\text{Lu}$ -BL01 was the highest in tumor, urinary bladder, liver, spleen, and skeleton. The spleen may be the dose-limiting organ for PRRT.<sup>95</sup>

**Other PRRT and PRS Mechanisms.** The imaging and therapy strategies described above are the most commonly applied in the present day, but scientists are still searching for new peptide tracers or targets which may provide unique

insights on certain diseases or provide better results for modern diagnostic methods and therapies. Zoghi et al. reported the new peptide tracer for PET imaging of gonadotropin-releasing hormone receptors (GnRH-R). These receptors are localized in normal and human cancer tissues including breast cancer. In addition, it was observed that GnRH-R are localized to a high percentage of estrogen receptor-negative breast cancers.<sup>96,97</sup> It is also known that GnRH-R agonists show an antiproliferative effect on breast cancer cells.<sup>98</sup> All this data was purposed for developing  $^{68}\text{Ga}$ -DOTA-triptorelin by Zoghi et al. as a novel radiolabeled peptide tracer in breast cancer diagnostic. They obtained 99% HPLC purity of the radiolabeled product after the full synthesis protocol. The biodistribution tests on normal rats provided data showing significant uptake in the kidney, stomach, and testicles, as well as fast kidney clearance. Furthermore, tests with T41 tumor-bearing mice provide information about significant tumor uptake 1 h after injection with a high value of tumor–blood and tumor–muscle ratios (28 and  $>50$ , respectively).<sup>99</sup> Another, less common radio-targeting strategy, is urokinase-type plasminogen receptors (uPARs) imaging. uPAR is a cell membrane protein responsible for proteolysis, but it also activates many intracellular signaling pathways, including proliferation through cooperation with transmembrane receptors. uPAR expression is limited in normal tissues, but uPAR overexpression was detected in cancer tissues, for example, in urinary bladder cancer and breast cancer. Moreover, it was reported that high uPAR expression is associated with cancer invasion and metastases. Therefore, uPAR is considered a biomarker for aggressive diseases and poor prognoses.<sup>100,101</sup> Skovsgaard et al. are working on the development of radioligands based on peptide uPAR antagonist AE105 for PET imaging. They reported the results of phase 1 clinical trial of  $^{68}\text{Ga}$ -NOTA-AE105, where they investigated its safety and biodistribution in normal tissues, as well as its uptake in tumor lesions. Ten patients with breast, prostate, and urinary bladder cancer took part in the trial. No patient experienced adverse events or clinically detectable pharmacologic effects due to administration of  $^{68}\text{Ga}$ -NOTA-AE105. Results indicated high in vivo stability, fast clearance from tissues, and primarily renal excretion of the radioligand. Image tests provided images with satisfactory contrast and allowed for identification of primary tumors and metastases. The most promising results were obtained for breast cancer patients, where the administration of  $^{68}\text{Ga}$ -NOTA-AE105 provided an image of localization of metastatic axillary lymph nodes, which has not been previously detected by preoperative workup with ultrasound, fine-needle aspiration, and contrast-enhanced CT. However, the scientist reported the failure of  $^{68}\text{Ga}$ -NOTA-AE105 PET in imaging liver metastasis in a patient with disseminated urinary bladder cancer.<sup>102</sup>

**RIT and RII Strategy.** Targeting radionuclides using monoclonal antibodies (Mabs) has been well studied in the literature. Identification of the acceptable antigen and selection of the proper MAB are paramount for obtaining successful therapies or diagnostic results. Antigens should be highly expressed in the targeted tissue, but not in other tissues, as this may affect the quality of imaging or therapy. In addition, they should be localized on the cell surface for accessibility to circulating Mabs. The properly selected antibody should be highly specific for the target antigen, while uptake in other tissues or cross activity with nonspecific antigens should be

low, because of the probability of occurrence of toxicity or excessively fast clearance.<sup>103</sup>

Nowadays there are a few kinds of Mabs used in medicine and a few methods of Mabs classification. In this review, we want to mention origin structure-type classification and include some information about production of these Mabs. The first type is murine Mabs produced by hybridoma cell lines. These are intact whole murine Mabs. It is the oldest and very widely used Mabs production technique. Names of these Mabs have several specific endings, e.g., –omab for mice antibodies, –emab for hamster antibodies, or –amab for rat antibodies, which makes these types of antibodies easy to recognize in praxis.<sup>104</sup> The second type are whole murine recombinant Mabs or Mabs fragments produced by cloning the genetic material responsible for expression of specific Mab fragments, creating a recombinant DNA chain, and using it in, for example, in yeast display or phage display system technology to obtain a specific product.<sup>105</sup> In addition, the recombinant Mabs can be basically divided into three subtypes. First subtype are chimeric Mabs. These are constructed mostly from human proteins (usually heavy chains, sometimes with light chain fragments) and murine proteins (light chains or only variable regions of light chains). All chimeric Mabs names ended in –ximab. The second subtype are humanized Mabs, where only the hypervariable region of human antibody has murine origin. These antibodies show reduced immunogenicity, because of reducing the human anti-mouse antibody production effect. Names of humanized Mabs end in –zumab.<sup>106</sup> The third subtype are human Mabs, which are constructed only from human proteins. Human Mabs are better tolerated by patients, and they eliminate the human anti-mouse antibody production effect. This type can be produced by recombinant techniques or by transgenic mice (specific modification of hybridoma cell lines technique). Human Mabs can be recognized by the –umab ending in the agent name.<sup>107</sup>

By analyzing recently reported studies, it is evident that scientists are focused on improving of immuno-PET technique in human therapy. This technique allows for the utilization of high specificity Mabs with the high sensitivity and resolution offered by PET imaging to perform noninvasive quantification of Mab uptake in normal and tumor tissues for therapy development. For example, it may be applied for the selection of targeted therapies or to choose the appropriate dose of radioimmunotherapy. Radiolabeling with positron emitting nuclides of therapeutic antitumor affibodies allows us to achieve theranostic goals such as the evaluation of responses to therapy.<sup>108,109</sup> ImmunoPET was utilized for evaluation of the impact of preloading with unlabeled rituximab on <sup>89</sup>Zr/<sup>90</sup>Y-rituximab radioimmunotherapy of CD20+ B-cell lymphoma. This study provided information about the impairment of radioconjugate tumor targeting in the majority of patients, which suggests the reconsideration and further evaluation of the preloading strategy in rituximab or <sup>90</sup>Y-ibritumomab tiuxetan therapy.<sup>110</sup> Pitalua-Cortez et al. successfully identified the overexpression of human epidermal growth factor receptor 2 (HER2) in lung metastases in a 43-year-old breast cancer patient by using immunoPET technique with <sup>68</sup>Ga radiolabeled trastuzumab. They compared the obtained image results with <sup>18</sup>F-FDG imaging. In conclusion, they confirmed that <sup>68</sup>Ga-trastuzumab provides information as a specific metastasis biomarker, but the higher uptake of <sup>18</sup>F-FDG and significant background activity of the liver and heart were caused by fast imaging after injection, because of the usage of a short-life

radionuclide, are the reasons for research continuation. Nevertheless, scientists pointed out that conjugation of Mabs with long-life radionuclides, which together have the capacity to improve image quality, may provide an excessively high radiation dose for the patient, because of slow blood clearance and the long residence time of Mabs.<sup>111</sup> One of the solutions to the biodistribution problem presented in the study performed by Pitalua-Cortez et al. is the modification of the peptide structure. Honarvar et al. developed a nonapeptide A9 derived from the trastuzumab-Fab portion, radiolabeled it with <sup>111</sup>In by using bifunctional chelator DTPA, and studied its affinity to HER2-expressing BT474 cells as well as biodistribution in NMRI mice. Binding to HER2-expressing cells study provided information about two interactions of <sup>111</sup>In-DTPA-A9 with HER2, specific for HER2 and nonspecific to characteristics for similar peptide structures. The biodistribution profile was also promising due to the substance's rapid clearance from blood and insignificant binding to any tissues.<sup>112</sup>

Another solution to solve pharmacokinetic problems was proposed by Xu et al. They modified a cysteinylated ZHER<sub>2,342</sub> anti-HER2 affibody with a hydrophilic linker and labeled it by the <sup>18</sup>FAl-NOTA method. Affibodies are a small size engineered scaffold protein binders (~6.5 kDa), originally based on the protein A domain. They are characterized by high affinity and very fast clearance of unbound molecules via the kidneys, because of their small size. A new tracer was developed named <sup>18</sup>FAl-NOTA-MAL-MZHER<sub>2,342</sub>. uPET imaging probes on mice provide very high image quality as confirmed by biodistribution studies. Results indicated rapid localization to HER2-positive tumors, quick elimination from blood and normal tissues, and low accumulation in liver or bones. <sup>18</sup>FAl-NOTA-MAL-MZHER<sub>2,342</sub> was excreted mainly through the kidney, and as a result, kidneys are the major dose-limiting organ. Scientists pointed out that renal protection could be used in future studies, and they declared an active investigation into the possible effects of these compounds.<sup>113</sup> Tolmachev et al. met with a different problem with renal excretion. They evaluated anti-HER2 affibody ZHER<sub>2,S1</sub> conjugated with NOTA and NODAGA chelators and radiolabeled with <sup>64</sup>Cu. These were compared with <sup>68</sup>Ga-NODAGA-ZHER<sub>2,S1</sub> to obtain information about which radionuclide is more favorable in immunoPET imaging of HER2-expressed tumors in mice. Results from biodistribution evaluation provided evidence of renal redistribution of the radiotracer. The renal uptake was reduced 6 and 24 h post injection and radioactivity increased in blood, lung, liver, spleen, and intestines at the same time. This resulted in a decrease of the tumor to organ ratio. In conclusion, Tolmachev et al. suggested avoiding the combination of radiocopper and NOTA/NODAGA amido derivatives with proteins displaying high renal reabsorption.<sup>114</sup> Sandberg et al. investigated a novel affibody, ABY-025, conjugated with <sup>68</sup>Ga and <sup>111</sup>In. ABY-025 is an affibody capable of identifying HER2 expression in breast cancer metastases. The radiolabeled molecule has successfully passed the first and second phases of clinical trials. In their study, Sandberg et al. successfully performed an intrimage normalization using tumor to reference tissue ratio by administration of <sup>68</sup>Ga-ABY-025 to 16 patients and <sup>111</sup>In-ABY-025 to 7 patients with prediagnosed HER2 positive/negative metastasized breast cancer and PET/CT or SPECT/CT scan, respectively.<sup>115</sup>

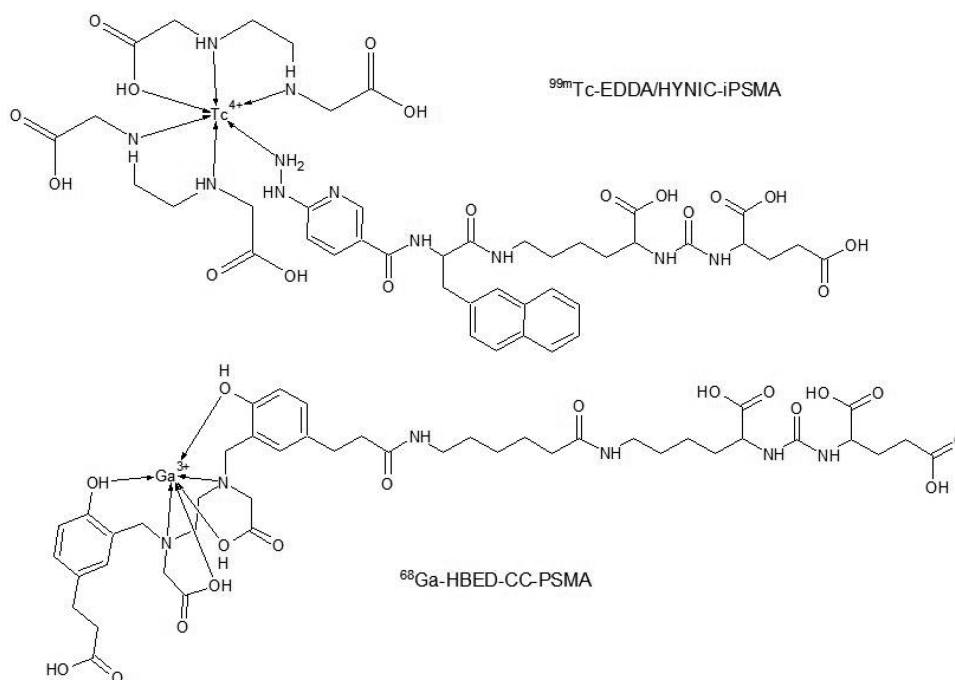


**Figure 5.** Schemes of PSMA derivatives applied in new diagnostic strategies.

The RIT or RII strategy is often associated with cancer, but not always.  $^{99m}\text{Tc}$ -labeled murine anti-human CD4 IgG1-Fab fragment were investigated by Steinhoff in patients with active synovitis due to rheumatoid arthritis to evaluate this compound as a potential marker of inflammatory activity. Study confirmed that scintigraphy with  $^{99m}\text{Tc}$ -anti-CD4-Fab is a promising technique.<sup>116</sup>

Recent immunoPET reports relate also to a new target—programed death-ligand 1 (PD-L1). It is an immune checkpoint in the negative regulation of T cells. Over-expression of PD-L1 was found in a variety of cancers and it is upregulated by tumors in the presence of infiltrating lymphocytes. Antibody blockage of PD-L1 was utilized to design therapeutic antibodies like the FDA-approved pembrolizumab, ipilimumab, and nivolumab. Mayer et al. developed four PD-L1 ligands radiolabeled with  $^{64}\text{Cu}$  and two radiolabeled with  $^{68}\text{Ga}$ . They used a small high-affinity consensus (HAC) PD1 peptide and its aglycosylated derivative (HACA) as a scaffold to design their radiotracers. They also evaluated the influence of chelators in their study. They used DOTA and NOTA chelators to conjugate the radionuclides in various structures. Results from immunoPET indicated that aglycolyzation was the most prominent design affecting tracer uptake, specificity, and clearance.  $^{64}\text{Cu}$ -NOTA-HACA-PD1 was an agent that visualized human PD-L1 expression as the most accurate in tumor bearing mice.  $^{68}\text{Ga}$ -DOTA-HACA-PD1 and  $^{68}\text{Ga}$ -NOTA-HACA-PD1 also exhibited a very promising tumor to background ratio 1 h post injection.<sup>117</sup>

Therapeutic application of radiolabeled antibodies has also been reported in recent literature. J591 is a murine Mab that has affinity to prostate-specific membrane antigen (PSMA) and has the property of internalization once bound to PSMA. PSMA is one of the most recognizable targets for management of castration-resistant prostate cancer (CRPC), and J591 was investigated for this application. Niaz et al. gathered the published clinical trials results of  $^{177}\text{Lu}$ -J591 in the treatment of CRPC.  $^{177}\text{Lu}$ -J591 application has shown promising results.

The agent targeted tumor accurately, gave biochemical and radiographical response, and increased overall survival among CRPC patients. Authors indicated that ongoing studies of  $^{177}\text{Lu}$ -J591 focus on improving the therapeutic index because of myelosuppression due  $^{177}\text{Lu}$ -J591 application.<sup>118</sup>

**Other Radiotargeting Strategies.** There are a number of strategies that cannot be assigned to PRRT or RIS, which are very widespread and are the mainstream in modern nuclear medicine science. The most popular technique in this division is prostate-specific membrane antigen (PSMA) imaging. PSMA is an integral membrane glycosylated metalloenzyme, and it is also known as glutamate carboxypeptidase II. It was found on the apical membrane of the epithelium lining the prostatic ducts in the healthy prostate, but it is also expressed in kidneys, liver, colon, and the nervous system. PSMA is of interest to the field of nuclear medicine because of its overexpression on prostate cancer cells. In addition, PSMA levels correlate well with the Gleason score, which makes PSMA a phenomenal target for identifying and monitoring the progression of prostate cancer.<sup>21</sup> Other tumors like gliomas or breast cancer are able to express PSMA also, and PSMA is then an angiogenesis marker.<sup>119</sup>

At present, the most common method for targeting PSMA is administration of the radiolabeled small urea-linked diamino acid ligand—the PSMA inhibitors (iPSMA). iPSMA may be radiolabeled with various radionuclides. Santos-Cuevas et al. evaluated the biokinetics of the conjugated iPSMA with  $^{99m}\text{Tc}$  by using the HYNIC/EDDA method as a SPECT or SPECT/CT, SPECT/MRI imaging agent in prostate cancer patients. They obtained high-resolution images of tumor and metastases through the use of SPECT/CT imaging, due to the high  $^{99m}\text{Tc}$ -EDDA/HYNIC-iPSMA (Figure 5) uptake in the prostate cancer tissue and metastases. Biokinetic studies on healthy volunteers confirmed the usefulness of this compound in human patients due to high patient tolerance after administration and a similar profile to the previously examined  $^{99m}\text{Tc}$ -iPSMA compounds. In addition,  $^{99m}\text{Tc}$ -EDDA/HYNIC-



iPSMA showed fast blood clearance and urinary excretion. Therefore, the scientists were able to perform the prostate cancer gland imaging 3 h after administration.<sup>120</sup> Advanced research on human patients was performed with <sup>68</sup>Ga-iPSMA-HBED-CC (Figure 5), also known as <sup>68</sup>Ga-PSMA11. Schmidt-Hegemann et al. performed a retrospective study of 129 prostate cancer patients in which <sup>68</sup>Ga-iPSMA-HBED-CC was used to visualize neoplastic lesions. Their aim was to define a pattern of positive lesion detection by using <sup>68</sup>Ga-iPSMA-HBED-CC PET/CT imaging. A few potential influencing factors were evaluated, and it was found that the level of prostate specific antigen in blood before PSMA–PET scan was significantly correlated with positive detection of lesions.<sup>121</sup> <sup>68</sup>Ga-iPSMA-HBED-CC is also considered as a potentially useful radiotracer in visualization of breast cancer metastasis, because of the reported PSMA expression on human solid tumors.<sup>122</sup> Minamimoto et al. compared the effectiveness of visualizing pathological lesions by PET/MRI and PET/CT with <sup>68</sup>Ga-RM (GRPR antagonist) and <sup>68</sup>Ga-iPSMA-HBED-CC, respectively, in patients with biochemically recurrent prostate cancer. Both radiotracers showed characteristic physiological uptake to specific organs. Uptake outside the expected physiologic biodistribution indicated a difference between agents. Administration of each agent allowed visualization of some lesions in bone marrow, retroperitoneal lymph nodes, mediastinal lymph nodes, seminal vesicle, and subclavian lymph nodes. However, <sup>68</sup>Ga-RM2 uptake was low in the pelvic lymph node and vas deferens, where <sup>68</sup>Ga-iPSMA-HBED-CC uptake was significantly higher. This phenomenon occurred twice in the same patients. Researchers also found lesions where <sup>68</sup>Ga-iPSMA-HBED-CC uptake was low in comparison to <sup>68</sup>Ga-RM2. In conclusion, studies by Minamimoto et al. indicate the need for advanced performance studies to understand the heterogeneous expression of PSMA and GRPRs in different types of prostate cancer.<sup>123</sup> In addition to many studies with <sup>68</sup>Ga-iPSMA-HBED-CC, the new radiolabeled iPSMA structures are reported. Liu et al. reported the synthesis and preclinical evaluation of <sup>68</sup>Ga-PSMA-BCH for prostate cancer imaging. It is a NOTA conjugated iPSMA structure and showed high affinity to 22Rv1 tumor cells expressing PSMA. Bouvet et al. evaluated the influence of prosthetic groups containing <sup>18</sup>F on tumor uptake in PSMA targeting. They investigated three new iPSMA structures conjugated with succinimidyl-4-[<sup>18</sup>F]fluorobenzoate (<sup>18</sup>F-SFB), 4-[<sup>18</sup>F]fluorobenzaldehyde (<sup>18</sup>F-FBA), and 2-deoxy-2-[<sup>18</sup>F]fluoro-D-glucose (<sup>18</sup>F-FDG) prosthetic groups. In vitro and in vivo studies indicated the iPSMA structure conjugated with <sup>18</sup>F-SFB prosthetic group as the most potent agent in future PSMA–PET imaging research.<sup>124</sup> iPSMA are also in interest of therapeutic applications.<sup>177</sup>Lu-iPSMA was reported as the beta emitting agent used in prostate cancer therapy and a good alternative to <sup>177</sup>Lu-J591, which is still being investigated and improved.<sup>125</sup> <sup>225</sup>Ac-iPSMA is new approach because of the usage of the alpha emitter. Alpha particles have greater destructive power against malignant cells than beta particles. Azorin-Vega et al. compared the effectiveness of <sup>177</sup>Lu-iPSMA and <sup>225</sup>Ac-iPSMA in a bone microenvironment model. Their studies proved that <sup>225</sup>Ac-iPSMA produced doses to prostate cancer cells almost 3 orders of magnitude greater than <sup>177</sup>Lu-iPSMA. Moreover, they indicated that <sup>225</sup>Ac-iPSMA could be the best option for treatment of the bone metastases in prostate cancer because of very high doses of radiation to prostate cancer cells in bone metastases.<sup>126</sup>

Another mechanism of tumor targeting was reported by Ahmadpour et al. They used a small synthetic tumor cell-binding peptide FROP-1 primarily reported by Zitzmann et al.<sup>127</sup> FROP-1 has an ability to bind specifically to MCF-7 breast tumor; therefore, Ahmadpour et al. conjugated FROP-1 peptide with HYNIC structure and radiolabeled it with <sup>99m</sup>Tc by using tricine and EDDA as a coligand. Planar gamma imaging in MCF-7 female tumor-bearing nude mice was acquired at 15 min after the administration of <sup>99m</sup>Tc-HYNIC-FROP. Tumors were clearly localized by SPECT imaging at 15 post injection also. Biodistribution studies indicated rapid blood clearance and renal excretion. Therefore, scientists observed a high radiation dose in kidneys and urinary bladder and found that radiolabeled FROP derivatives needed further studies in order to improve in vivo tumor targeting.<sup>128</sup>

## ■ CLINICAL TRIAL ANALYSIS

For the purposes of this publication, a review of clinical trials on the use of new radiolabeled peptide structures in therapy or diagnostics was performed. The review refers to studies reported on [www.clinicaltrials.gov](http://www.clinicaltrials.gov) in the period from 2008 to November 31, 2018, and it includes 146 trials involving the use of radiolabeled peptide structures in medicine. The complete list of analyzed clinical trials is presented in Table S1. Among them, 28 had the status of terminated, withdrawn, or unknown. Out of the 50 trials completed, three trials concerned phase 3 of clinical trials. They were the safety and efficacy study of <sup>111</sup>In pentetate in high doses in treatment of neuroendocrine tumors (NCT00442533), the comparison of rituximab versus tositumomab and <sup>131</sup>I tositumomab in patients with relapsed follicular nonhodgkins lymphoma (NCT00268983), and a study on the impact of adding <sup>90</sup>Y ibritumomab tiuxetan to BEAM chemotherapy and autologous stem-cell transplantation in patients with aggressive lymphoma (NCT00491491). Other completed trials concerned phase 1 and phase 2, and included 23 and 24 trials, respectively. A significant majority of the trials concerned the RIT strategy (86.00%) and pretargeted RIT strategy (8.00%) where bispecific antibodies are used. Only one completed clinical trial was performed for diagnostic purposes, and this was phase 2 of a clinical trial study on the use <sup>68</sup>Ga-DOTA-RM2 PET/MRI in diagnostic imaging in patients with prostate cancer (NCT02440308). Seventeen active clinical trials were found. No active phase 3 trials were found; however, one phase 0 of a clinical trial was reported. This was the pilot clinical trial study on the use <sup>99</sup>Tc HYNIC/Tricine Interleukin-2 in SPECT imaging in patients with stage IV skin melanoma (NCT01789827). This study also was the only active clinical trial performed for diagnostic purposes. In this group of trials, RIT (76.47%) and pretargeted RIT (11.76%) were also the most often studied strategy of therapy. Forty-seven clinical trials have a recruiting status, of which five trials concerned phase 3 clinical trials. The goal of the diagnostic phase 3 trial was to determine the effectiveness of PET/MRI imaging in detection of prostate cancer cells with <sup>68</sup>Ga DOTA-RM2 in patients with negative CT scan and elevated prostate-specific antigen levels after surgical treatment or radiation (NCT02624518). Two phase 3 clinical trials concerned PRRT strategy. They were studies of the efficacy and safety of use <sup>177</sup>Lu-DOTATOC in patients with inoperable, progressive, somatostatin receptor-positive GEP-NET (NCT03049189) and studies of the use of <sup>111</sup>In pentetate-based adjuvant therapy in patients with digestive neuro-

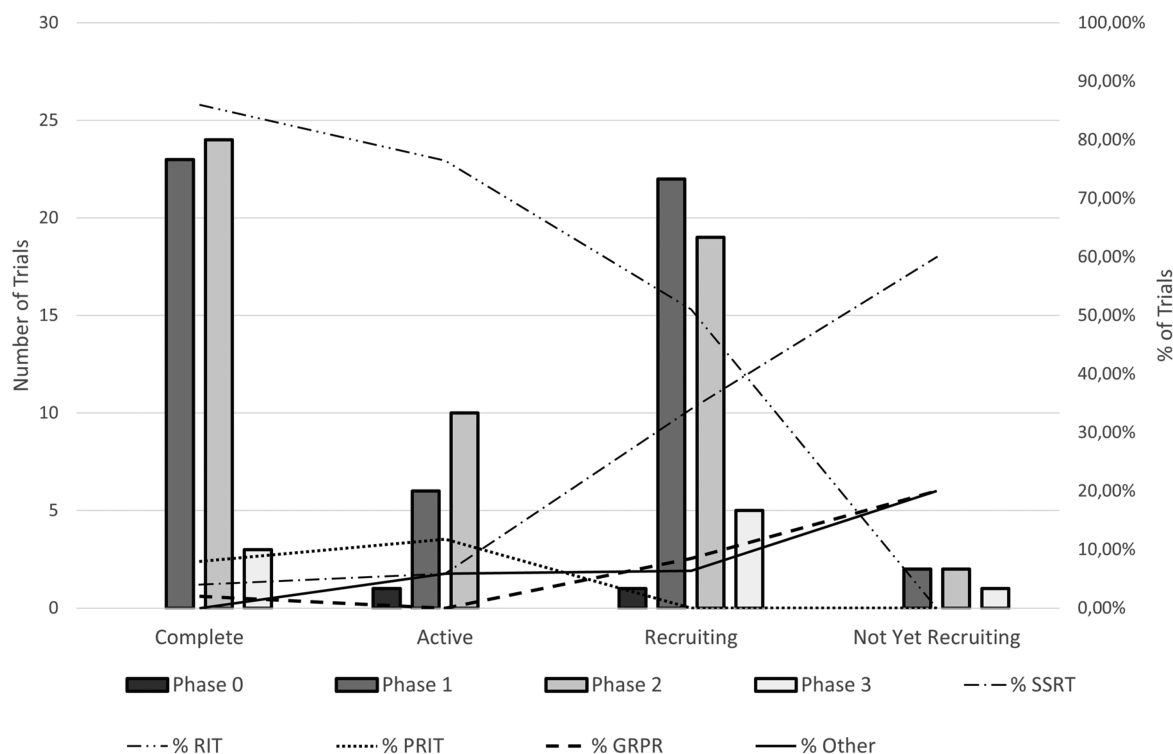


Figure 6. Summary of clinical trial analysis.

endocrine tumors after complete surgical resection of liver metastases (NCT02465112). The last two phase 3 clinical trials with a recruiting status concerned RIT strategy. Those were studies on the use of intracerebroventricular treatment with  $^{131}\text{I}$  omburtamab in children with diagnosed neuroblastoma and central nervous system/leptomeningeal metastases (NCT03275402) and studies of the comparison of  $^{90}\text{Y}$  ibritumomab tiuxetan RIT to autologous stem cell transplantation in patients with relapsed or refracted follicular lymphoma (NCT01827605). One pilot phase 0 clinical trial was reported as a trial at a recruitment stage. It concerned evaluation of the use  $^{64}\text{Cu}$  anticarcinoembryonic (CEA) antigen monoclonal antibody MSA in PET imaging of CEA positive cancer (NCT02293954). Clinical trials with a recruiting status mainly concerned treatment procedures; only ten trials were reported as studies with a diagnostic primary purpose. RIT strategy was also the most common strategy of studies in this group of trials (51.06%); however, PRRT was the second most frequently reported treatment strategy (34.04%). Four trials were reported as clinical trials in a prerecruitment stage. One of them was a phase 3 diagnostic clinical trial, where the examination of the performance of the LightPath Imaging System combined with  $^{68}\text{Ga}$  DOTA-RM2 as PET tracer was planned (NCT03731026). A two-phase diagnostic clinical trial involving studies of  $^{68}\text{Ga}$  DOTA-TATE as PET/MRI tracer of hepatocellular carcinoma (NCT03648073) was also identified as a trial in a prerecruitment stage. Graphical summary of clinical trial analysis is shown in Figure 6.

## SUMMARY

In conclusion, the most actively studied therapy with radiolabeled peptides in the period from 2008 to November 31, 2018 was radioimmunotherapy. The majority of completed and active clinical trials performed in that period were aimed at

application of radiolabeled antibodies. New clinical trials that will commence soon or in which the recruitment process will begin are also concerned with radiolabeled antibodies. Nevertheless, the number of studies with somatostatin and bombesin analogues has increased. It is noteworthy that these new phase 3 clinical trials were more than complete and active, which brings hope for new radiolabeled peptide agents in modern therapy and diagnosis.

## ASSOCIATED CONTENT

### Supporting Information

The Supporting Information is available free of charge at <https://pubs.acs.org/doi/10.1021/acs.bioconjchem.0c00617>.

List of clinical trials (PDF)

## AUTHOR INFORMATION

### Corresponding Author

Paweł Szymański – Department of Pharmaceutical Chemistry, Drug Analyses and Radiopharmacy, Faculty of Pharmacy, Medical University of Lodz, 90-151 Lodz, Poland; [orcid.org/0000-0003-3438-7509](https://orcid.org/0000-0003-3438-7509); Email: [pawel.szymanski@umed.lodz.pl](mailto:pawel.szymanski@umed.lodz.pl)

### Authors

Paweł Kręcisz – Department of Pharmaceutical Chemistry, Drug Analyses and Radiopharmacy, Faculty of Pharmacy, Medical University of Lodz, 90-151 Lodz, Poland; [orcid.org/0000-0003-2951-0867](https://orcid.org/0000-0003-2951-0867)

Kamila Czarnecka – Department of Pharmaceutical Chemistry, Drug Analyses and Radiopharmacy, Faculty of Pharmacy, Medical University of Lodz, 90-151 Lodz, Poland; [orcid.org/0000-0002-6497-1565](https://orcid.org/0000-0002-6497-1565)

Leszek Królicki – Department of Nuclear Medicine, Medical University of Warsaw, 02-097 Warsaw, Poland;

orcid.org/0000-0002-7117-9621

Elżbieta Mikiciuk-Olasik – Department of Pharmaceutical Chemistry, Drug Analyses and Radiopharmacy, Faculty of Pharmacy, Medical University of Lodz, 90-151 Lodz, Poland; orcid.org/0000-0002-7171-4524

Complete contact information is available at:

<https://pubs.acs.org/10.1021/acs.bioconjchem.0c00617>

### Author Contributions

All authors have given approval to the final version of the manuscript.

### Notes

The authors declare no competing financial interest.

### REFERENCES

- (1) Richter, S., and Wuest, F. (2014) F-18-Labeled Peptides: The Future Is Bright. *Molecules* 19 (12), 20536–20556.
- (2) Krenning, E. P., Breeman, W. A. P., Kooij, P. P. M., Lameris, J. S., Bakker, W. H., Koper, J. W., Ausema, L., Reubi, J. C., and Lamberts, S. W. J. (1989) LOCALIZATION OF ENDOCRINE-RELATED TUMORS WITH RADIOIODINATED ANALOG OF SOMATOSTATIN. *Lancet* 333 (8632), 242–244.
- (3) Muto, P., Latoria, S., Varrella, P., Vergara, E., Salvatore, M., Morgano, G., ListerJames, J., Bernardy, J. D., Dean, R. T., Wencker, D., et al. (1995) Detecting Deep Venous Thrombosis with Tc-99m-Labeled Synthetic Peptide P280. *J. Nucl. Med.* 36 (8), 1384–1391.
- (4) ListerJames, J., Knight, L. C., Maurer, A. H., Bush, L. R., Moyer, B. R., and Dean, R. T. (1996) Thrombus imaging with a technetium-99m-labeled, activated platelet receptor-binding peptide. *J. Nucl. Med.* 37 (5), 775–781.
- (5) de Visser, M., Verwijnen, S. M., and de Jong, M. (2008) Improvement strategies for peptide receptor scintigraphy and radionuclide therapy. *Cancer Biother.Radiopharm.* 23 (2), 137–157.
- (6) Goldenberg, D. M., Sharkey, R. M., Paganelli, G., Barbet, J., and Chatal, J. F. (2006) Antibody pretargeting advances cancer radioimmunodetection and radioimmunotherapy. *J. Clin. Oncol.* 24 (5), 823–834.
- (7) Leaman Alcibar, O., Candini, D., Lopez-Campos, F., Albert Antequera, M., Morillo Macias, V., Conde, A. J., Rodriguez Perez, A., Hervas Moron, A., Contreras Martinez, J., Ferrer Albiach, C., Navarro Aguilar, S., Rodriguez-Ruiz, M. E., et al. (2019) Time for radioimmunotherapy: an overview to bring improvements in clinical practice. *Clin. Transl. Oncol.* 21 (8), 992–1004.
- (8) Jacobson, O., Zhu, L., Ma, Y., Weiss, I. D., Sun, X. L., Niu, G., Kiesewetter, D. O., and Chen, X. Y. (2011) Rapid and Simple One-Step F-18 Labeling of Peptides. *Bioconjugate Chem.* 22 (3), 422–428.
- (9) Tolmachev, V., and Stone-Elander, S. (2010) Radiolabelled proteins for positron emission tomography: Pros and cons of labelling methods. *Biochim. Biophys. Acta, Gen. Subj.* 1800 (5), 487–510.
- (10) Marek, M. J., Lambert, C. R., and Rhodes, B. A. (1994) TECHNIQUES FOR DIRECT RADIOLABELING OF MONOCLONAL-ANTIBODIES. *Radiolabeled Blood Elements: Recent Advances in Techniques and Applications* 262, 207–220.
- (11) Greenland, W. E. P., and Blower, P. J. (2005) Water-soluble phosphines for direct labeling of peptides with technetium and rhenium: Insights from electrospray mass spectrometry. *Bioconjugate Chem.* 16 (4), 939–948.
- (12) Wilbur, D. S. (1992) Radiohalogenation of Proteins - an Overview of Radionuclides, Labeling Methods, And Reagents for Conjugate Labeling. *Bioconjugate Chem.* 3 (6), 433–470.
- (13) Kiesewetter, D. O., Jacobson, O., Lang, L. X., and Chen, X. Y. (2011) Automated radiochemical synthesis of F-18 FBEM: A thiol reactive synthon for radiofluorination of peptides and proteins. *Appl. Radiat. Isot.* 69 (2), 410–414.
- (14) Vaidyanathan, G., and Zalutsky, M. R. (1992) Labeling proteins with fluorine-18 using N-succinimidyl 4-[18F]fluorobenzoate. *International Journal of Radiation Applications and Instrumentation. Part B. Nuclear Medicine and Biology* 19 (3), 275–281.
- (15) Guhlke, S., Coenen, H. H., and Stöcklin, G. (1994) Fluoroacylation agents based on small n.c.a. [18F]fluorocarboxylic acids. *Appl. Radiat. Isot.* 45 (6), 715–727.
- (16) Basuli, F., Zhang, X., Phelps, T. E., Jagoda, E. M., Choyke, P. L., and Swenson, R. E. (2020) Automated Synthesis of Fluorine-18 Labeled CXCR4 Ligand via the Conjugation with Nicotinic AcidN-Hydroxysuccinimide Ester (6- F-18 SFPy). *Molecules* 25 (17), 3924.
- (17) Meyer, J. P., Adumeau, P., Lewis, J. S., and Zeglis, B. M. (2016) Click Chemistry and Radiochemistry: The First 10 Years. *Bioconjugate Chem.* 27 (12), 2791.
- (18) Sachin, K., Jadhav, V. H., Kim, E. M., Kim, H. L., Lee, S. B., Jeong, H. J., Lim, S. T., Sohn, M. H., and Kim, D. W. (2012) F-18 Labeling Protocol of Peptides Based on Chemically Orthogonal Strain-Promoted Cycloaddition under Physiologically Friendly Reaction Conditions. *Bioconjugate Chem.* 23 (8), 1680–1686.
- (19) McBride, W. J., D'Souza, C. A., Sharkey, R. M., Karacay, H., Rossi, E. A., Chang, C. H., and Goldenberg, D. M. (2010) Improved F-18 Labeling of Peptides with a Fluoride-Aluminum-Chelate Complex. *Bioconjugate Chem.* 21 (7), 1331–1340.
- (20) Schibli, R., and Schubiger, P. A. (2002) Current use and future potential of organometallic radiopharmaceuticals. *Eur. J. Nucl. Med. Mol. Imaging* 29 (11), 1529–1542.
- (21) Jackson, I. M., Scott, P. J. H., and Thompson, S. (2017) Clinical Applications of Radiolabeled Peptides for PET. *Semin. Nucl. Med.* 47 (5), 493–523.
- (22) Eder, M., Krivoshein, A. V., Backer, M., Backer, J. M., Haberkorn, U., and Eisenhut, M. (2010) ScVEGF-PEG-HBED-CC and scVEGF-PEG-NOTA conjugates: comparison of easy-to-label recombinant proteins for Ga-68 PET imaging of VEGF receptors in angiogenic vasculature. *Nucl. Med. Biol.* 37 (4), 405–412.
- (23) Maecke, H. R., and André, J. P. (2007) *68Ga-PET Radiopharmacy: A Generator-Based Alternative to 18F-Radiopharmacy*, Berlin, Heidelberg, pp 215–242, Springer Berlin Heidelberg, Berlin, Heidelberg.
- (24) Brouwers, A. H., van Eerd, J. E. M., Frielink, C., Oosterwijk, E., Oyen, W. J. G., Corstens, F. H. M., and Boerman, O. C. (2004) Optimization of radioimmunotherapy of renal cell carcinoma: Labeling of monoclonal antibody cG250 with I-131, Y-90, Lu-177, or Re-186. *J. Nucl. Med.* 45 (2), 327–337.
- (25) Psimadas, D., Georgoulis, P., Valotassiou, V., and Loudos, G. (2012) Molecular Nanomedicine Towards Cancer: In-111-Labeled Nanoparticles. *J. Pharm. Sci.* 101 (7), 2271–2280.
- (26) Borjesson, P. K. E., Jauw, Y. W. S., Boellaard, R., de Bree, R., Comans, E. F. I., Roos, J. C., Castelijns, J. A., Vosjan, M., Kummer, J. A., Leemans, C. R., et al. (2006) Performance of immuno-positron emission tomography with zirconium-89-labeled chimeric monoclonal antibody U36 in the detection of lymph node metastases in head and neck cancer patients. *Clin. Cancer Res.* 12 (7), 2133–2140.
- (27) Meszaros, L. K., Dose, A., Biagini, S. C. G., and Blower, P. J. (2010) Hydrazinonicotinic acid (HYNIC) - Coordination chemistry and applications in radiopharmaceutical chemistry. *Inorg. Chim. Acta* 363 (6), 1059–1069.
- (28) Meszaros, L. K., Dose, A., Biagini, S. C. G., and Blower, P. J. (2011) Synthesis and evaluation of analogues of HYNIC as bifunctional chelators for technetium. *Dalton Transactions* 40 (23), 6260–6267.
- (29) Charron, C. L., Hickey, J. L., Nsima, T. K., Cruickshank, D. R., Turnbull, W. L., and Luyt, L. G. (2016) Molecular imaging probes derived from natural peptides. *Nat. Prod. Rep.* 33 (6), 761–800.
- (30) Decristoforo, C., and Mather, S. J. (1999) 99m-technetium-labelled peptide-HYNIC conjugates: Effects of lipophilicity and stability on biodistribution. *Nucl. Med. Biol.* 26 (4), 389–396.
- (31) Qaim, S. M. (2019) Theranostic radionuclides: recent advances in production methodologies. *J. Radioanal. Nucl. Chem.* 322 (3), 1257–1266.



- (32) Berman, D. S., Kiat, H., Van Train, K., Friedman, J. D., Wang, F. P., and Germano, G. (1994) Dual-Isotope Myocardial Perfusion Spect with Rest Thallium-201 and Stress Tc-99m Sestamibi. *Cardiology Clinics* 12 (2), 261–270.
- (33) Rangger, C., and Haubner, R. (2020) Radiolabelled Peptides for Positron Emission Tomography and Endoradiotherapy in Oncology dagger. *Pharmaceuticals* 13 (2), 22.
- (34) Feijtel, D., de Jong, M., and Nonnekens, J. (2020) Peptide Receptor Radionuclide Therapy: Looking Back, Looking Forward. *Curr. Top. Med. Chem.* 20, 2959.
- (35) Vaidyanathan, G., and Zalutsky, M. R. (2008) Astatine Radiopharmaceuticals: Prospects and Problems. *Curr. Radiopharm.* 1 (3), 177–177.
- (36) Sharifi, M., Jalilian, A. R., Yousefnia, H., Alirezapour, B., Bahrami-Samani, A., and Zolghadri, S. (2018) Production, quality control, biodistribution and imaging studies of Lu-177-PSMA-617 in breast adenocarcinoma model. *Radiochim. Acta* 106 (6), 507–513.
- (37) Fani, M., Nicolas, G. P., and Wild, D. (2017) Somatostatin Receptor Antagonists for Imaging and Therapy. *J. Nucl. Med.* 58, 61S–66S.
- (38) Sharma, N., Naraev, B. G., Engelman, E. G., Zimmerman, M. B., Bushnell, D. L., O'Doriso, T. M., O'Doriso, M. S., Menda, Y., Muller-Brand, J., Howe, J. R., et al. (2017) Peptide Receptor Radionuclide Therapy Outcomes in a North American Cohort With Metastatic Well-Differentiated Neuroendocrine Tumors. *Pancreas* 46 (2), 151–156.
- (39) Veliky, I., Sundin, A., Eriksson, B., Lundqvist, H., Sorensen, J., Bergstrom, M., and Langstrom, B. (2010) In vivo binding of Ga-68-DOTATOC to somatostatin receptors in neuroendocrine tumours - impact of peptide mass. *Nucl. Med. Biol.* 37 (3), 265–275.
- (40) Hardiansyah, D., Attarwala, A. A., Kletting, P., Mottaghy, F. M., and Glattig, G. (2017) Prediction of time-integrated activity coefficients in PRRT using simulated dynamic PET and a pharmacokinetic model. *Physica Medica-European Journal of Medical Physics* 42, 298–304.
- (41) Hardiansyah, D., Maass, C., Attarwala, A. A., Muller, B., Kletting, P., Mottaghy, F. M., and Glattig, G. (2016) The role of patient-based treatment planning in peptide receptor radionuclide therapy. *Eur. J. Nucl. Med. Mol. Imaging* 43 (5), 871–880.
- (42) Hardiansyah, D., Guo, W., Kletting, P., Mottaghy, F. M., and Glattig, G. (2016) Time-integrated activity coefficient estimation for radionuclide therapy using PET and a pharmacokinetic model: A simulation study on the effect of sampling schedule and noise. *Med. Phys.* 43 (9), 5145–5154.
- (43) Bergsma, H., van Lom, K., Konijnenberg, M., Kam, B., Teunissen, J., de Herder, W., Krenning, E., and Jkwেকেboom, D. (2018) Therapy-related hematological malignancies after peptide receptor radionuclide therapy with 177 Lu-DOTA-Octreotate: Incidence, course & predicting factors in patients with GEP-NETS. *J. Nucl. Med.* 59, 452.
- (44) Hervas, I., Bello, P., Falgas, M., del Olmo, M. I., Torres, I., Olivas, C., Vera, V., Olivan, P., and Yepes, A. M. (2017) Lu-177-DOTATATE treatment in neuroendocrine tumours. A preliminary study. *Revista Espanola De Medicina Nuclear E Imagen Molecular* 36 (2), 91–98.
- (45) Gospavic, R., Knoll, P., Mirzaei, S., and Popov, V. (2016) Physiologically Based Pharmacokinetic (PBPK) Model for Biodistribution of Radiolabeled Peptides in Patients with Neuroendocrine Tumours. *Asia Oceania journal of nuclear medicine & biology* 4 (2), 90–97.
- (46) Clift, A. K., Giele, H., Reddy, S., Macedo, R., Al-Nahas, A., Wasan, H. S., Gondolesi, G. E., Vianna, R. M., Friend, P., Vaidya, A., et al. (2017) Neoadjuvant peptide receptor radionuclide therapy and modified multivisceral transplantation for an advanced small intestinal neuroendocrine neoplasm: an updated case report. *Innovative Surgical Sciences* 2 (4), 247.
- (47) Zemczak, A., Kołodziej, M., Gut, P., Królicki, L., Kos-Kudła, B., Kamiński, G., Ruchala, M., Pawlak, D., and Kunikowska, J. (2020) Effect of Peptide Receptor Radionuclide Therapy (PRRT) with tandem isotopes -  $[^{90}\text{Y}]/[^{177}\text{Lu}]$ Lu-DOTATATE in patients with disseminated neuroendocrine tumours depending on qualification  $[^{18}\text{F}]\text{FDG}$  PET/CT in Polish multicenter experience - do we need  $[^{18}\text{F}]\text{FDG}$ . *Endokrynol. Pol.*, 1 DOI: 10.5603/EP.a2020.0014.
- (48) Kunikowska, J., Zemczak, A., Kołodziej, M., Gut, P., Lon, I., Pawlak, D., Mikolajczak, R., Kaminski, G., Ruchala, M., Kos-Kudła, B., and Krolicki, L. (2020) Tandem peptide receptor radionuclide therapy using Y-90/Lu-177-DOTATATE for neuroendocrine tumors efficacy and side-effects-polish multicenter experience. *Eur. J. Nucl. Med. Mol. Imaging* 47 (4), 922–933.
- (49) Berzaczy, D., Giraudo, C., Haug, A. R., Raderer, M., Senn, D., Karanikas, G., Weber, M., and Mayerhoefer, M. E. (2017) Whole-Body  $^{68}\text{Ga}$ -DOTANOC PET/MRI Versus  $^{68}\text{Ga}$ -DOTANOC PET/CT in Patients With Neuroendocrine Tumors: A Prospective Study in 28 Patients. *Clinical Nuclear Medicine* 42 (9), 669–674.
- (50) Ginj, M., Zhang, H. W., Waser, B., Cescato, R., Wild, D., Wang, X. J., Ercegyi, J., Rivier, J., Macke, H. R., and Reubi, J. C. (2006) Radiolabeled somatostatin receptor antagonists are preferable to agonists for in vivo peptide receptor targeting of tumors. *Proc. Natl. Acad. Sci. U. S. A.* 103 (44), 16436–16441.
- (51) Dalm, S. U., Nonnekens, J., Doeswijk, G. N., de Blois, E., van Gent, D. C., Konijnenberg, M. W., and de Jong, M. (2016) Comparison of the Therapeutic Response to Treatment with a Lu-177-Labeled Somatostatin Receptor Agonist and Antagonist in Preclinical Models. *J. Nucl. Med.* 57 (2), 260–265.
- (52) Wild, D., Fani, M., Fischer, R., Del Pozzo, L., Kaul, F., Krebs, S., Rivier, J. E. F., Reubi, J. C., Maecke, H. R., and Weber, W. A. (2014) Comparison of Somatostatin Receptor Agonist and Antagonist for Peptide Receptor Radionuclide Therapy: A Pilot Study. *J. Nucl. Med.* 55 (8), 1248–1252.
- (53) Nicolas, G. P., Mansi, R., McDougall, L., Kaufmann, J., Bouterfa, H., Wild, D., and Fani, M. (2017) Biodistribution, Pharmacokinetics, and Dosimetry of Lu-177-, Y-90-, and In-111-Labeled Somatostatin Receptor Antagonist OPS201 in Comparison to the Agonist Lu-177-DOTATATE: The Mass Effect. *J. Nucl. Med.* 58 (9), 1435–1441.
- (54) Dalm, S. U., Haeck, J., Doeswijk, G. N., de Blois, E., de Jong, M., and van Deurzen, C. H. M. (2017) SSTR-Mediated Imaging in Breast Cancer: Is There a Role for Radiolabeled Somatostatin Receptor Antagonists? *J. Nucl. Med.* 58 (10), 1609–1614.
- (55) Morgat, C., Mishra, A. K., Varshney, R., Allard, M., Fernandez, P., and Hindie, E. (2014) Targeting Neuropeptide Receptors for Cancer Imaging and Therapy: Perspectives with Bombesin, Neurotensin, and Neuropeptide-Y Receptors. *J. Nucl. Med.* 55 (10), 1650–1657.
- (56) Ramos-Alvarez, I., Moreno, P., Mantey, S. A., Nakamura, T., Nuche-Berenguer, B., Moody, T. W., Coy, D. H., and Jensen, R. T. (2015) Insights into bombesin receptors and ligands: Highlighting recent advances. *Peptides* 72, 128–144.
- (57) Morgat, C., MacGrogan, G., Brouste, V., Velasco, V., Sevenet, N., Bonnefoi, H., Fernandez, P., Debled, M., and Hindie, E. (2017) Expression of Gastrin-Releasing Peptide Receptor in Breast Cancer and Its Association with Pathologic, Biologic, and Clinical Parameters: A Study of 1,432 Primary Tumors. *J. Nucl. Med.* 58 (9), 1401–1407.
- (58) Bodei, L., Ferrari, M., Nunn, A., Llull, J., Cremonesi, M., Martano, L., Laurora, G., Scardino, E., Tiberini, S., Bufi, G., et al. (2007) Lu-177-AMBA Bombesin analogue in hormone refractory prostate cancer patients: A phase I escalation study with single-cycle administrations. *European Journal of Nuclear Medicine and Molecular Imaging* 34, S221–S221.
- (59) Nock, B. A., Kaloudi, A., Lymperis, E., Giarika, A., Kulkarni, H. R., Klette, I., Singh, A., Krenning, E. P., de Jong, M., Maina, T., et al. (2017) Theranostic Perspectives in Prostate Cancer with the Gastrin Releasing Peptide Receptor Antagonist NeoBOMB1: Preclinical and First Clinical Results. *J. Nucl. Med.* 58 (1), 75–80.
- (60) Kaloudi, A., Lymperis, E., Giarika, A., Dalm, S., Orlandi, F., Barbato, D., Tedesco, M., Maina, T., de Jong, M., and Nock, B. A. (2017) NeoBOMB1, a GRPR-Antagonist for Breast Cancer Theragnostics: First Results of a Preclinical Study with Ga-67

NeoBOMB1 in T-47D Cells and Tumor-Bearing Mice. *Molecules* 22 (11), 1950.

(61) Dalm, S. U., Bakker, I. L., de Blois, E., Doeswijk, G. N., Konijnenberg, M. W., Orlandi, F., Barbato, D., Tedesco, M., Maina, T., Nock, B. A., and de Jong, M. (2017) Ga-68/Lu-177-NeoBOMB1, a Novel Radiolabeled GRPR Antagonist for Theranostic Use in Oncology. *J. Nucl. Med.* 58 (2), 293–299.

(62) Cheng, S. Y., Lang, L. X., Wang, Z. T., Jacobson, O., Yung, B., Zhu, G. Z., Gu, D. Y., Ma, Y., Zhu, X. H., Niu, G., et al. (2018) Positron Emission Tomography Imaging of Prostate Cancer with Ga-68-Labeled Gastrin-Releasing Peptide Receptor Agonist BBN7–14 and Antagonist RM26. *Bioconjugate Chem.* 29 (2), 410–419.

(63) Liolios, C., Buchmuller, B., Bauder-Wust, U., Schafer, M., Leotta, K., Haberkorn, U., Eder, M., and Kopka, K. (2018) Monomeric and Dimeric Ga-68-Labeled Bombesin Analogues for Positron Emission Tomography (PET) Imaging of Tumors Expressing Gastrin-Releasing Peptide Receptors (GRPRs). *J. Med. Chem.* 61 (5), 2062–2074.

(64) Taherian, A., Li, X. L., Liu, Y. Q., and Haas, T. A. (2011) Differences in integrin expression and signaling within human breast cancer cells. *BMC Cancer* 11, 15.

(65) Jin, H., and Varner, J. (2004) Integrins: roles in cancer development and as treatment targets. *Br. J. Cancer* 90 (3), 561–565.

(66) Li, Z. B., Chen, K., and Chen, X. (2008) Ga-68-labeled multimeric RGD peptides for microPET imaging of integrin alpha(v)beta(3) expression. *Eur. J. Nucl. Med. Mol. Imaging* 35 (6), 1100–1108.

(67) Ortiz-Arzate, Z., Santos-Cuevas, C. L., Ocampo-Garcia, B. E., Ferro-Flores, G., Garcia-Becerra, R., Estrada, G., Gomez-Argumosa, E., and Izquierdo-Sanchez, V. (2014) Kit preparation and biokinetics in women of Tc-99m-EDDA/HYNIC-E-c(RGDfK) (2) for breast cancer imaging. *Nucl. Med. Commun.* 35 (4), 423–432.

(68) Janssen, M., Oyen, W. J. G., Massuger, L., Frielink, C., Dijkgraaf, I., Edwards, D. S., Radjopadhye, M., Corstens, F. H. M., and Boerman, O. C. (2002) Comparison of a monomeric and dimeric radiolabeled RGD-peptide for tumor targeting. *Cancer Biother. Radiopharm.* 17 (6), 641–646.

(69) Zhang, J. J., Mao, F., Niu, G., Peng, L., Lang, L. X., Li, F., Ying, H. Y., Wu, H. W., Pan, B. J., Zhu, Z. H., et al. (2018) Ga-68-BBN-RGD PET/CT for GRPR and Integrin alpha(v)beta(3) Imaging in Patients with Breast Cancer. *Theranostics* 8 (4), 1121–1130.

(70) Kazmierczak, P. M., Todica, A., Gildehaus, F. J., Hirner-Eppeneder, H., Brendel, M., Eschbach, R. S., Hellmann, M., Nikolaou, K., Reiser, M. F., Wester, H. J., et al. (2016) Ga-68-TRAP-(RGD)(3) Hybrid Imaging for the In Vivo Monitoring of alpha(v)beta(3)-Integrin Expression as Biomarker of Anti-Angiogenic Therapy Effects in Experimental Breast Cancer. *PLoS One* 11 (12), 19.

(71) Brubaker, P. L., and Drucker, D. J. (2004) Minireview: Glucagon-like peptides regulate cell proliferation and apoptosis in the pancreas, gut, and central nervous system. *Endocrinology* 145 (6), 2653–2659.

(72) Willard, F. S., and Sloop, K. W. (2012) Physiology and Emerging Biochemistry of the Glucagon-Like Peptide-1 Receptor. *Exp. Diabetes Res.* 2012, 12.

(73) Azad, B. B., Rota, V., Yu, L. H., McGirr, R., Amant, A. H. S., Lee, T. Y., Dhanvantari, S., and Luyt, L. G. (2015) Synthesis and Evaluation of Optical and PET GLP-1 Peptide Analogues for GLP-1R Imaging. *Mol. Imaging* 14, 16.

(74) Wild, D., Macke, H., Christ, E., Gloor, B., and Reubi, J. C. (2008) Glucagon-like peptide 1-receptor scans to localize occult insulinomas. *N. Engl. J. Med.* 359 (7), 766–768.

(75) Christ, E., Wild, D., Forrer, F., Brandl, M., Sahli, R., Clerici, T., Gloor, B., Martius, F., Maecke, H., and Reubi, J. C. (2009) Glucagon-Like Peptide-1 Receptor Imaging for Localization of Insulinomas. *J. Clin. Endocrinol. Metab.* 94 (11), 4398–4405.

(76) Bauman, A., Valverde, I. E., Fischer, C. A., Vomstein, S., and Mindt, T. L. (2015) Development of Ga-68- and Zr-89-Labeled Exendin-4 as Potential Radiotracers for the Imaging of Insulinomas by PET. *J. Nucl. Med.* 56 (10), 1569–1574.

(77) Antwi, K., Fani, M., Heye, T., Nicolas, G., Rottenburger, C., Kaul, F., Merkle, E., Zech, C. J., Boll, D., Vogt, D. R., et al. (2018) Comparison of glucagon-like peptide-1 receptor (GLP-1R) PET/CT, SPECT/CT and 3T MRI for the localisation of occult insulinomas: evaluation of diagnostic accuracy in a prospective crossover imaging study. *Eur. J. Nucl. Med. Mol. Imaging* 45 (13), 2318–2327.

(78) Parihar, A. S., Vadi, S. K., Kumar, R., Mittal, B. R., Singh, H., Bal, A., Walia, R., Shukla, J., and Sinha, S. K. (2018) 68Ga DOTA-Exendin PET/CT for Detection of Insulinoma in a Patient With Persistent Hyperinsulinemic Hypoglycemia. *Clinical Nuclear Medicine* 43 (8), E285–E286.

(79) Kirsi, M., Cheng-Bin, Y., Veronica, F., Tamiko, I., Viki-Veikko, E., Johan, R., Jori, J., Tiina, S., Tuula, T., Marko, T., Eleni, G., Martin, B., Martin, G., Claude, R. J., Helmut, M., Anne, R., Olof, S., Pirjo, N., et al. (2014) Cu-64- and Ga-68-Labeled Nle(14),Lys(40)(Ahx-NODAGA)NH<sub>2</sub>-Exendin-4 for Pancreatic Beta Cell Imaging in Rats. *Molecular Imaging and Biology* 16 (2), 255–263.

(80) Li, J. F., Rawson, J., Chea, J., Tang, W., Miao, L., Sui, F., Li, L., Poku, E., Shively, J. E., and Kandeel, F. (2019) Evaluation of Ga-68 DO3A-VS-Cys(40)-Exendin-4 as a PET Probe for Imaging Human Transplanted Islets in the Liver. *Sci. Rep.* 9, 8.

(81) Wang, L. Z., Liu, Y., Xu, Y. P., Sheng, J., Pan, D. H., Wang, X. Y., Yan, J. J., Yang, R. L., and Yang, M. (2018) Age-related change of GLP-1R expression in rats can be detected by F-18 AIF-NOTA-MAL-Cys(39)-exendin-4. *Brain Res.* 1698, 213–219.

(82) Juarez, J., Bendall, L., and Bradstock, K. (2004) Chemokines and their receptors as therapeutic targets: The role of the SDF-1/CXCR4 axis. *Curr. Pharm. Des.* 10 (11), 1245–1259.

(83) Kircher, M., Herhaus, P., Schottelius, M., Buck, A. K., Werner, R. A., Wester, H. J., Keller, U., and Lapa, C. (2018) CXCR4-directed theranostics in oncology and inflammation. *Ann. Nucl. Med.* 32 (8), 503–511.

(84) Feng, Y., Broder, C. C., Kennedy, P. E., and Berger, E. A. (1996) HIV-1 entry cofactor: Functional cDNA cloning of a seven-transmembrane, G protein-coupled receptor. *Science* 272 (5263), 872–877.

(85) Nagafuchi, Y., Shoda, H., Sumitomo, S., Nakachi, S., Kato, R., Tsuchida, Y., Tsuchiya, H., Sakurai, K., Hanata, N., Tateishi, S., et al. (2016) Immunophenotyping of rheumatoid arthritis reveals a linkage between HLA-DRB1 genotype, CXCR4 expression on memory CD4(+) T cells, and disease activity. *Sci. Rep.* 6, 11.

(86) Galkina, E., and Ley, K. (2009) Immune and Inflammatory Mechanisms of Atherosclerosis. *Annu. Rev. Immunol.* 27, 165–197.

(87) Fang, H. Y., Munch, N. S., Schottelius, M., Ingermann, J., Liu, H. B., Schauer, M., Stangl, S., Multhoff, G., Steiger, K., Gerngross, C., et al. (2018) CXCR4 Is a Potential Target for Diagnostic PET/CT Imaging in Barrett's Dysplasia and Esophageal Adenocarcinoma. *Clin. Cancer Res.* 24 (5), 1048–1061.

(88) Bonham, L. W., Karch, C. M., Fan, C. C., Tan, C., Geier, E. G., Wang, Y., Wen, N., Broce, I. J., Li, Y., Barkovich, M. J., et al. (2018) CXCR4 involvement in neurodegenerative diseases. *Transl. Psychiatry* 8, 10.

(89) Demmer, O., Gourni, E., Schumacher, U., Kessler, H., and Wester, H. J. (2011) PET Imaging of CXCR4 Receptors in Cancer by a New Optimized Ligand. *ChemMedChem* 6 (10), 1789–1791.

(90) Wester, H. J., Keller, U., Schottelius, M., Beer, A., Philipp-Abbrederis, K., Hoffmann, F., Simecek, J., Gerngross, C., Lassmann, M., Herrmann, K., et al. (2015) Disclosing the CXCR4 Expression in Lymphoproliferative Diseases by Targeted Molecular Imaging. *Theranostics* 5 (6), 618–630.

(91) Breun, M., Monoranu, C. M., Kessler, A. F., Matthies, C., Lohr, M., Hagemann, C., Schirbel, A., Rowe, S. P., Pomper, M. G., Buck, A. K., et al. (2019) Ga-68 -Pentixafor PET/CT for CXCR4-Mediated Imaging of Vestibular Schwannomas. *Front. Oncol.* 9, 6.

(92) Wang, Z., Zhang, M. R., Wang, L., Wang, S. J., Kang, F., Li, G. Q., Jacobson, O., Niu, G., Yang, W. D., Wang, J., et al. (2015) Prospective Study of Ga-68-NOTA-NFB: Radiation Dosimetry in Healthy Volunteers and First Application in Glioma Patients. *Theranostics* 5 (8), 882–889.

- (93) Yan, X. F., Niu, G., Wang, Z., Yang, X. Y., Kiesewetter, D. O., Jacobson, O., Shen, B. Z., and Chen, X. Y. (2016) Al F-18 NOTA-T140 Peptide for Noninvasive Visualization of CXCR4 Expression. *Molecular Imaging and Biology* 18 (1), 135–142.
- (94) Schottelius, M., Osl, T., Poschenrieder, A., Hoffmann, F., Beykan, S., Hanscheid, H., Schirbel, A., Buck, A. K., Kropf, S., Schwaiger, M., et al. (2017) Lu-177 pentixather: Comprehensive Preclinical Characterization of a First CXCR4-directed Endoradiotherapeutic Agent. *Theranostics* 7 (9), 2350–2362.
- (95) Lau, J., Kwon, D., Rousseau, E., Zhang, Z. X., Zeisler, J., Uribe, C. F., Kuo, H. T., Zhang, C. C., Lin, K. S., and Benard, F. (2019) Ga-68 Ga/Lu-177 Lu-BL01, a Novel Theranostic Pair for Targeting C-X-C Chemokine Receptor 4. *Mol. Pharmaceutics* 16 (11), 4688–4695.
- (96) Fekete, M., Wittliff, J. L., and Schally, A. V. (1989) Characteristics and Distribution of Receptors for D-Trp6-Luteinizing Hormone-Releasing Hormone, Somatostatin, Epidermal Growth-Factor, And Sex Steroids in 500 Biopsy Samples of Human-Breast Cancer. *J. Clin. Lab. Anal.* 3 (3), 137–147.
- (97) Eidne, K. A., Flanagan, C. A., Harris, N. S., and Millar, R. P. (1987) Gonadotropin-Releasing-Hormone (Gnrh)-Binding Sites in Human-Breast Cancer Cell-Lines and Inhibitory Effects of Gnrh Antagonists. *J. Clin. Endocrinol. Metab.* 64 (3), 425–432.
- (98) Fekete, M., Zalutnai, A., Comaruschally, A. M., and Schally, A. V. (1989) Membrane-Receptors for Peptides in Experimental and Human Pancreatic Cancers. *Pancreas* 4 (5), 521–528.
- (99) Zoghi, M., Jalilian, A. R., Niazi, A., Johari-Daha, F., Alirezapour, B., and Ramezanzpour, S. (2016) Development of a Ga-68-peptide tracer for PET GnRH1-imaging. *Ann. Nucl. Med.* 30 (6), 400–408.
- (100) Dohn, L. H., Pappot, H., Iversen, B. R., Illemann, M., Hoyer-Hansen, G., Christensen, I. J., Thind, P., Salling, L., von der Maase, H., and Laerum, O. D. (2015) uPAR Expression Pattern in Patients with Urothelial Carcinoma of the Bladder - Possible Clinical Implications. *PLoS One* 10 (8), 15.
- (101) Persson, M., and Kjaer, A. (2013) Urokinase-type plasminogen activator receptor (uPAR) as a promising new imaging target: potential clinical applications. *Clin. Physiol. Funct. Imaging* 33 (5), 329–337.
- (102) Skovgaard, D., Persson, M., Brandt-Larsen, M., Christensen, C., Madsen, J., Klausen, T. L., Holm, S., Andersen, F. L., Loft, A., Berthelsen, A. K., et al. (2017) Safety, Dosimetry, and Tumor Detection Ability of Ga-68-NOTA-AE105: First-in-Human Study of a Novel Radioligand for uPAR PET Imaging. *J. Nucl. Med.* 58 (3), 379–386.
- (103) Carmon, K. S., and Azhdarinia, A. (2018) Application of Immuno-PET in Antibody-Drug Conjugate Development. *Mol. Imaging* 17, 10.
- (104) Keenan, A. M., Harbert, J. C., and Larson, S. M. (1985) Monoclonal-Antibodies in Nuclear-Medicine. *J. Nucl. Med.* 26 (5), 531–537.
- (105) Siegel, D. L. (2002) Recombinant monoclonal antibody technology. *Transfusion Clinique Et Biologique* 9 (1), 15–22.
- (106) Benjouad, A. (2009) Antibody biotechnology. *African Journal of Biotechnology* 8 (13), 2911–2915.
- (107) Lonberg, N., and Huszar, D. (1995) Human Antibodies from Transgenic Mice. *Int. Rev. Immunol.* 13 (1), 65–93.
- (108) Bailly, C., Clery, P. F., Favier-Chauvet, A., Bourgeois, M., Guerard, F., Haddad, F., Barbet, J., Cherel, M., Kraeber-Bodere, F., Carlier, T., et al. (2017) Immuno-PET for Clinical Theranostic Approaches. *Int. J. Mol. Sci.* 18 (1), 57.
- (109) Bodet-Milin, C., Bailly, C., Toucheffeu, Y., Frampas, E., Bourgeois, M., Rauscher, A., Lacoueille, F., Drui, D., Arlicot, N., Goldenberg, D. M., et al. (2019) Clinical Results in Medullary Thyroid Carcinoma Suggest High Potential of Pretargeted Immuno-PET for Tumor Imaging and Theranostic Approaches. *Front. Med.* 6, 7.
- (110) Muylle, K., Flamen, P., Vugts, D., Guiot, T., Ghanem, G., Meuleman, N., Bourgeois, P., Vanderlinden, B., van Dongen, G., Everaert, H., et al. (2015) Tumour targeting and radiation dose of radioimmunotherapy with Y-90-rituximab in CD20+B-cell lymphoma as predicted by Zr-89-rituximab immuno-PET: impact of preloading with unlabelled rituximab. *Eur. J. Nucl. Med. Mol. Imaging* 42 (8), 1304–1314.
- (111) Pitalua-Cortes, Q. G., Garcia-Perez, F. O., Villasenor-Navarro, Y., Lara-Medina, F. U., Matus-Santos, J. A., Soldevilla-Gallardo, I., Porras-Reyes, F. I., Perez-Sanchez, V. M., Maldonado-Martinez, H. A., Perez-Baez, W., et al. (2017) Ga-68-DTPA Anti-HER2 positron emission tomography/CT successfully predicts the overexpression of human epidermal growth factor receptor in lung metastases from breast cancer. *Bjr Case Reports* 3 (3), 20160136.
- (112) Honarvar, H., Calce, E., Doti, N., Langella, E., Orlova, A., Buijs, J., D'Amato, V., Bianco, R., Saviano, M., Tolmachev, V., et al. (2018) Evaluation of HER2-specific peptide ligand for its employment as radiolabeled imaging probe. *Sci. Rep.* 8, 12.
- (113) Xu, Y. P., Bai, Z. C., Huang, Q. H., Pan, Y. Y., Pan, D. H., Wang, L. Z., Yan, J. J., Wang, X. Y., Yang, R. L., and Yang, M. (2017) PET of HER2 Expression with a Novel (FAL)-F-18 Labeled Affibody. *J. Cancer* 8 (7), 1170–1178.
- (114) Tolmachev, V., Yim, C. B., Rajander, J., Perols, A., Karlstrom, A. E., Haaparanta-Solin, M., Gronroos, T. J., Solin, O., and Orlova, A. (2017) Comparative Evaluation of Anti-HER2 Affibody Molecules Labeled with Cu-64 Using NOTA and NODAGA. *Contrast Media Mol. Imaging* 2017, 1.
- (115) Sandberg, D., Tolmachev, V., Veliky, I., Olofsson, H., Wennborg, A., Feldwisch, J., Carlsson, J., Lindman, H., and Sorensen, J. (2017) Intra-image referencing for simplified assessment of HER2-expression in breast cancer metastases using the Affibody molecule ABY-025 with PET and SPECT. *Eur. J. Nucl. Med. Mol. Imaging* 44 (8), 1337–1346.
- (116) Steinhoff, K., Pierer, M., Siegert, J., Pigla, U., Laub, R., Hesse, S., Seidel, W., Sorger, D., Seese, A., Kuenstler, J. U., et al. (2014) Visualizing inflammation activity in rheumatoid arthritis with Tc-99 m Anti-CD4-mAb fragment scintigraphy. *Nucl. Med. Biol.* 41 (4), 350–354.
- (117) Mayer, A. T., Natarajan, A., Gordon, S. R., Maute, R. L., McCracken, M. N., Ring, A. M., Weissman, I. L., and Gambhir, S. S. (2017) Practical Immuno-PET Radiotracer Design Considerations for Human Immune Checkpoint Imaging. *J. Nucl. Med.* 58 (4), 538–546.
- (118) Niaz, M. O., Sun, M., Ramirez-Fort, M., and Niaz, M. J. (2020) Review of Lutetium-177-labeled Anti-prostate-specific Membrane Antigen Monoclonal Antibody J591 for the Treatment of Metastatic Castration-resistant Prostate Cancer. *Cureus* 12 (2), 6.
- (119) Nomura, N., Pastorino, S., Jiang, P. F., Lambert, G., Crawford, J. R., Gymnopoulos, M., Piccioni, D., Juarez, T., Pingle, S. C., Makale, M., et al. (2014) Prostate specific membrane antigen (PSMA) expression in primary gliomas and breast cancer brain metastases. *Cancer Cell Int.* 14, 26.
- (120) Santos-Cuevas, C., Davanzo, J., Ferro-Flores, G., Garcia-Perez, F. O., Ocampo-Garcia, B., Ignacio-Alvarez, E., Gomez-Argumosa, E., and Pedraza-Lopez, M. (2017) Tc-99m-labeled PSMA inhibitor: Biokinetics and radiation dosimetry in healthy subjects and imaging of prostate cancer tumors in patients. *Nucl. Med. Biol.* 52, 1–6.
- (121) Schmidt-Hegemann, N. S., Fendler, W. P., Buchner, A., Stief, C., Rogowski, P., Niyazi, M., Eze, C., Li, M. L., Bartenstein, P., Belka, C., and Ganswindt, U. (2017) Detection level and pattern of positive lesions using PSMA PET/CT for staging prior to radiation therapy. *Radiat. Oncol.* 12, 9.
- (122) Sathegke, M., Lengana, T., Modiselle, M., Vorster, M., Zeevaart, J., Maes, A., Ebenhan, T., and Van de Wiele, C. (2017) Ga-68-PSMA-HBED-CC PET imaging in breast carcinoma patients. *Eur. J. Nucl. Med. Mol. Imaging* 44 (4), 689–694.
- (123) Minamimoto, R., Hancock, S., Schneider, B., Chin, F. T., Jamali, M., Loening, A., Vasanawala, S., Gambhir, S. S., and Iagaru, A. (2016) Pilot Comparison of Ga-68-RM2 PET and Ga-68-PSMA-11 PET in Patients with Biochemically Recurrent Prostate Cancer. *J. Nucl. Med.* 57 (4), 557–562.
- (124) Bouvet, V., Wuest, M., Bailey, J. J., Bergman, C., Janzen, N., Valliant, J. F., and Wuest, F. (2017) Targeting Prostate-Specific Membrane Antigen (PSMA) with F-18-Labeled Compounds: the



Influence of Prosthetic Groups on Tumor Uptake and Clearance Profile. *Molecular Imaging and Biology* 19 (6), 923–932.

(125) Baum, R. P., Kulkarni, H. R., Schuchardt, C., Singh, A., Wirtz, M., Wiessalla, S., Schottelius, M., Mueller, D., Klette, I., and Wester, H. J. (2016) Lu-177-Labeled Prostate-Specific Membrane Antigen Radioligand Therapy of Metastatic Castration-Resistant Prostate Cancer: Safety and Efficacy. *J. Nucl. Med.* 57 (7), 1006–1013.

(126) Azorin-Vega, E., Rojas-Calderon, E., Ferro-Flores, G., Aranda-Lara, L., Jimenez-Mancilla, N., and Nava-Cabrera, M. A. (2019) Assessment of the radiation absorbed dose produced by Lu-177-iPSMA, Ac-225-iPSMA and (RaCl<sub>2</sub>)-Ra-223 to prostate cancer cell nuclei in a bone microenvironment model. *Appl. Radiat. Isot.* 146, 66–71.

(127) Zitzmann, S., Kramer, S., Mier, W., Hebling, U., Altmann, A., Rother, A., Berndorff, D., Eisenhut, M., and Haberkorn, U. (2007) Identification and evaluation of a new tumor cell-binding peptide, FROP-1. *J. Nucl. Med.* 48 (6), 965–972.

(128) Ahmadvour, S., Noaparast, Z., Abedi, S. M., and Hosseinimehr, S. J. (2018) Tc-99m-HYNIC-(tricine/EDDA)-FROP peptide for MCF-7 breast tumor targeting and imaging. *J. Biomed. Sci.* 25, 11.